Technische Universität München
TUM School of Medicine and Health

Redirecting T cell specificity by targeted integration of a tumor-reactive T cell receptor into the *TRAC* locus

Julian Josef Albers

Vollständiger Abdruck der von der TUM School of Medicine and Health der Technischen Universität München zur Erlangung eines Doktors der Medizinischen Wissenschaft (Dr. med. sci.) genehmigten Dissertation.

Vorsitz: Prof. Dr. Dirk H. Busch / Prof. Dr. Florian Eyer

Prüfende der Dissertation:

1. Prof. Dr. Angela Krackhardt
2. Prof. Dr. Radu Roland Rad
3. Prof. Dr. Sebastian Kobold

Die Dissertation wurde am 18.01.2024 bei der Technischen Universität München eingereicht und durch die TUM School of Medicine and Health am 05.06.2024 angenommen.

Table of Contents

Parts of this thesis have already been published:

„Gene editing enables T-cell engineering to redirect antigen specificity for potent tumor rejection“

Julian J Albers, Tim Ammon, Dario Gosmann, Stefan Audehm, Silvia Thoene, Christof Winter, Ramona Secci, Anja Wolf, Anja Stelzl, Katja Steiger, Jürgen Ruland, Florian Bassermann, Christian Kupatt, Martina Anton, Angela M Krackhardt

Life Sci Alliance, 2(2). doi:10.26508/lsa.201900367 (2019)

Abbreviations

4-1BB	TNF receptor superfamily member 9 (TNFRSF9), CD137
AAV	Adeno-associated Virus
AAV2	Adeno-associated virus serotype 2
AAV6	Adeno-associated virus serotype 6
ACT	Adoptive cell transfer
allo-HSCT	allogeneic hematopoietic stem cell transplantations
AML	Acute myeloid leukemia
BCMA	B-cell maturation antigen
bp	Base pairs
BSA	Bovine serum albumin
CAR	Chimeric antigen receptor
Cas9	CRISPR associated protein 9
CMV	Cytomegalovirus
CR	Complete remission
CRISPR	Clustered Regularly Interspaced Short Palindromic Repeats
crRNA	CRISPR RNA
DAB	3,3'-Diaminobenzidine
ddPCR	Digital-droplet PCR
DEPC	Diethyl pyrocarbonate
DMEM	Dulbecco's Modified Eagle Medium
DMSO	Dimethylsulfoxide
DNA	Deoxyribonucleic acid
DPBS	Dulbecco's phosphate-buffered saline
DSB	double-strand break
dsDNA	double-stranded DNA
EDTA	Ethylenediaminetetraacetic acid
EF1α	Eukaryotic Translation Elongation Factor 1 Alpha 1
EIF2C1	Eukaryotic Translation Initiation Factor 2C 1, Argonaute RISC Component 1
ELISA	Enzyme-linked Immunosorbent Assay
FA	Fanconi anemia
FACS	Fluorescence Activated Cell Sorting
FCS	Fetal calf serum
FDA	U.S. Food and Drug Administration
FISH	Fluorescence in situ hybridization
fluc	Firefly luciferase
GMP	Good manufacturing practice
gRNA	guideRNA
HDR	Homology-directed repair
HE	Hematoxylin and eosin stain
HEPES	Hydroxyethylpiperazine ethane sulfonic acid
HLA	Human leukocyte antigen
HSC	hematopoietic stem cell

HSCT	hematopoietic stem cell transplantation
IFN-γ	Interferon gamma
IL	Interleukin
indels	insertions or deletions
ITR	Inverted terminal repeat
J-segment	Joining segment
LHA	Left homology arm
MCS	Multiple cloning site
MHC	Major histocompatibility complex
MMEJ	Microhomology-mediated end joining
MOI	Multiplicity of infection
mRNA	Messenger RNA
N.T.	non-targeting
NHEJ	Nonhomologous end joining
NMD	Nonsense-mediated decay
NY-ESO-1	New York esophageal squamous cell carcinoma 1
P2A	Peptide 2A
p53	Transformation-related protein 53 (TRP53)
PAM	Protospacer adjacent motif
PBMC	Peripheral blood mononuclear cell
PCR	Polymerase chain reaction
PD1	Programmed cell death protein 1
PFA	Paraformaldehyde
PHACTR1	phosphatase and actin regulator 1
PT	promoter trap
qPCR	Real-time quantitative polymerase chain reaction
r/r B-NHL	relapsed/refractory B cell non-Hodgkin lymphoma
RHA	Right homology arm
RNA	Ribonucleic acid
RNP	Ribonucleoprotein
RV-TCR	retrovirally transferred TCR
scFv	Single-chain variable fragment
SCID-X1	X-linked severe combined immunodeficiency
sgRNA	single-guideRNA
siRNA	Small interfering RNA
SpCas9	*Streptococcus pyogenes* Cas9
ssDNA	Singe-strand DNA
TALENs	Transcription Activator-like Effector Nucleases
T_{CM}	T central memory cells
T_{SCM}	T memory stem cells
TCR	T cell receptor
TCRendo^{-}	Knock-out of the endogenous TCR
TCRhuman	human αβ-TCR
TCRmu	murinized αβ-TCR

TLA	Targeted locus amplification
TRAC	T Cell Receptor Alpha Constant
tracrRNA	Trans-activating crRNA
TRBC	T Cell Receptor Beta Constant
TRBC1	T Cell Receptor Beta Constant 1
TRBC2	T Cell Receptor Beta Constant 2
V-segment	Variable segment
VCN	Vector-copy number
ZFN	Zinc finger nuclease

List of Figures

List of Tables

Summary

Immunotherapies against cancer have led to impressive clinical results in some patients. Among those therapies, the adoptive transfer of T cell receptor (TCR) transgenic T cells holds tremendous potential for highly specific, personalized cancer treatment. For adoptive T cell transfer (ACT), T cells are harvested, genetically engineered to express a transgenic tumor-reactive TCR, expanded *ex vivo*, and transfused to the patients. In this project, we established the targeted integration of a tumor-reactive TCR gene (TCR2.5D6) into the T Cell Receptor Alpha Constant (*TRAC*) locus and investigated how the mode of genetic modification affects the T cell product.

Commonly, semi-randomly integrating vectors – such as γ-retroviral vectors, lentiviral vectors, or transposons – are used to insert the transgene encoding the tumor-reactive TCR into T cells that already express an endogenous TCR. This has several potential drawbacks: (1) Transgene integration is not targeted and carries the genotoxic risk of insertional mutagenesis. (2) Difficulties arise from the expression of the TCR chains of two different TCRs in one cell. The endogenous TCR chains compete for surface expression and can potentially form autoreactive mispaired TCRs with the chains of the introduced TCR. (3) Moreover, the transcription of the introduced TCR is controlled by a strong exogenous promoter. This promoter may be functionally inferior to the endogenous gene regulatory network that regulates transcription of the endogenous TCR-α chain.

To circumvent these problems, we used CRISPR-Cas9 Ribonucleoproteins (RNPs) and recombinant Adeno-associated Viruses serotype 6 (AAV6) to integrate the tumor-reactive TCR2.5D6 into the *TRAC* locus of primary human T cells (TCR knock-in). This simultaneously introduces the transgene and disrupts the expression of the endogenous TCR α-chain. Using a promoter-trap mechanism, we placed the introduced TCR2.5D6 under the transcriptional control of the endogenous *TRAC* gene-regulatory network.

Our data demonstrate that the knock-in of a tumor-reactive TCR into the *TRAC* locus is possible and exchanges the surface-expressed TCR of the edited T cells. This redirects T cells against antigen-bearing tumor cells *in vitro* and allows them to effectively reject a xenograft tumor in

an *in vivo* mouse model. In our experimental setup, we did not detect any functional differences between TCR knock-in T cells, in which the introduced TCR is regulated by the endogenous *TRAC* promoter, and retrovirally transduced T cells, in which the transgene is controlled by an exogenous MPSV-LTR promoter.

In light of our results and the findings of others, the benefits of targeted CRISPR-Cas9-mediated TCR integration can be evaluated in a more nuanced manner: While the transgene is reliably integrated into the target site, the genotoxic side effects of CRISPR-Cas9 in clinical translation need further investigation. Furthermore, in many cases, it is necessary to disrupt both the endogenous *TRAC* and T Cell Receptor Beta Constant (*TRBC*) loci to entirely eliminate competition and mispairing with endogenous TCR chains. Ultimately, long-term *in vivo* studies and results from clinical *in-patient* trials will reveal which form of transcriptional regulation of the introduced TCR is optimal for potent and durable anti-tumor responses. The targeted integration of transgenes into T cells has meanwhile been methodologically developed significantly and is being applied in initial clinical studies.

Zusammenfassung

Immuntherapien gegen Krebs haben bei einigen Patient*innen zu beeindruckenden klinischen Resultaten geführt. Der adoptive Transfer von T-Zell-Rezeptor (TZR)-transgenen T-Zellen hat enormes Potential für eine hochspezifische, personalisierte Krebsbehandlung. Beim adoptiven T-Zell-Transfer (AZT) werden T-Zellen entnommen, gentechnisch so verändert, dass sie einen transgenen tumorreaktiven TZR exprimieren, *ex vivo* expandiert und dann den Patient*innen transfundiert. In diesem Projekt etablierten wir die zielgerichtete Integration eines tumorreaktiven TZR-Gens in den Genlokus der konstanten Region der T-Zell-Rezeptor Alpha-Kette (*TRAC* Lokus) und untersuchten, wie die Art der gentechnischen Veränderung das T-Zellprodukt beeinflusst.

Üblicherweise werden semi-zufällig integrierende Vektoren, wie etwa γ-retrovirale Vektoren, lentivirale Vektoren oder Transposons, verwendet, um das Transgen, das für den tumorreaktiven TZR kodiert, in T-Zellen einzubauen, die bereits einen endogenen TZR exprimieren. Dies bringt einige Nachteile mit sich: (1) Die Transgen-Integration ist nicht zielgerichtet und birgt das genotoxische Risiko der Insertionsmutagenese. (2) Schwierigkeiten ergeben sich aus der Expression der T-Zell-Rezeptor-Ketten von zwei verschiedenen TZRs in einer Zelle. Die endogenen TZR-Ketten konkurrieren um die Oberflächenexpression und können mit den Ketten des eingeführten TZR potenziell autoreaktive fehlgepaarte TZRs bilden. (3) Zudem wird die Transkription des eingeführten TZR von einem starken exogenen Promotor gesteuert. Dieser Promotor könnte dem endogenen Genregulationsnetzwerk, das die Transkription der endogenen TZR-α-Kette reguliert, funktionell unterlegen sein.

Um diese Probleme zu umgehen, verwendeten wir CRISPR-Cas9-Ribonukleoproteine (RNPs) und rekombinante Adeno-assoziierte Viren des Serotyps 6 (AAV6), um den tumorreaktiven TZR2.5D6 in den *TRAC*-Lokus primärer menschlicher T-Zellen zu integrieren (TZR Knock-in). Dadurch wird gleichzeitig das Transgen eingeführt und die Expression der endogenen TZR-α-Kette unterbrochen. Mithilfe eines Promoter-Trap Mechanismus stellten wir das eingeführte TZR2.5D6 unter die transkriptionelle Kontrolle des endogenen *TRAC*-Genregulationsnetzwerks.

Unsere Daten zeigen, dass der Knock-in eines tumorreaktiven TZR in den *TRAC*-Lokus möglich ist und den TZR, den die T-Zellen an der Oberfläche exprimieren, austauscht. Dadurch werden die T-Zellen *in vitro* gegen antigentragende Tumorzellen gerichtet und stoßen *in vivo* einen Xenograft-Tumor in einem Mausmodell wirksam ab. In unserem Versuchsaufbau konnten wir keine funktionellen Unterschiede zwischen TZR-Knock-in-T-Zellen, bei denen der TZR durch den endogenen *TRAC*-Promoter reguliert wird, und retroviral transduzierten T-Zellen, bei denen das Transgen durch einen exogenen MPSV-LTR Promoter gesteuert wird, feststellen.

In Anbetracht unserer Ergebnisse und der Erkenntnisse anderer Arbeitsgruppen können die Vorteile der gezielten CRISPR-Cas9-vermittelten TZR-Integration differenzierter beurteilt werden: Während das Transgen zuverlässig in die Zielstelle integriert wird, müssen die genotoxischen Nebenwirkungen von CRISPR-Cas9 in der klinischen Umsetzung weiter untersucht werden. Darüber hinaus ist es in vielen Fällen notwendig, sowohl den endogenen *TRAC*- als auch den *TRBC*-Lokus auszuschalten, um Konkurrenz und Fehlpaarungen mit endogenen TZR-Ketten vollständig zu unterbinden. Letztendlich werden langfristige *in vivo* Studien und die Ergebnisse klinischer Studien an Patienten zeigen, welche Form der transkriptionellen Kontrolle des eingebrachten TZR eine wirksame und dauerhafte Tumorkontrolle ermöglicht. Die gezielte Integration von Transgenen in T Zellen wurde methodisch inzwischen deutlich weiterentwickelt und wird aktuell in ersten klinischen Studien erprobt.

1. Introduction

1.1 Adoptive T cell transfer – development of a “living drug”

Successfully defeating human tumors requires a complex multicellular immune response, the elements and interactions of which are only partially understood (Hanahan, 2022; Hanahan & Weinberg, 2011; Mellman, Chen, Powles, & Turley, 2023). The essential role of T cells in this response has long been established (Waldman, Fritz, & Lenardo, 2020). Among a broad range of therapeutic approaches aimed at enhancing T-cell mediated tumor cell killing, adoptive T-cell transfer (ACT) stands out as an approach using cells as a “living drug” with exquisite therapeutic responses in some cancer entities (June & Sadelain, 2018; Lim & June, 2017).

Historically, early studies demonstrated that infiltrated T cells could be isolated from tumors (TILs), expanded ex vivo, and readministered, which led to impressive responses in some patients, especially for patients with malignant melanoma (Rosenberg et al., 1988). While constituting an essential proof-of-principle, this therapy proved challenging to scale up. In an allogenic setting, donor-lymphocyte infusions in patients receiving allogeneic hematopoietic stem cell transplantations (allo-HSCT) showed promising anti-tumor effects, termed the graft-versus-leukemia effect (Bonini, Chapuis, Hudecek, Guedan, Magnani, & Qasim, 2023; Collins et al., 1997; Kolb et al., 1990). The ability to genetically transfer antigen-receptor genes to harvested peripheral T cells, however, significantly improved the efficiency and clinical scalability of the therapy and allowed the usage of novel, synthetic tumor-reactive receptors to redirect the T cells’ specificity (Morgan et al., 2006; Rosenberg et al., 1990). This ultimately led to the approval of six adoptive T–cell therapies at the time of this writing (Bonini et al., 2023).

1.2 Tumor-reactive antigen receptors: CARs and transgenic TCRs

Two kinds of antigen receptors are commonly transferred to therapeutic T cells to redirect the specificity against tumor cells: Chimeric antigen receptors (CARs) and transgenic T cell receptors (TCRs).

CARs are synthetic receptors that combine an antibody's recognition ability with the signaling ability of a TCR. The fusion protein consists of an extracellular Single-chain variable fragment

(scFv) or two nanobody heavy chains (Vhh) for antigen recognition, linked to a transmembrane domain, an intracellular CD3ζ signaling domain, and additional co-stimulatory elements such as 4-1BB or CD28 (Labanieh & Mackall, 2023). With the antigen-recognition domain, CARs detect surface structures on target cells in a Major histocompatibility complex (MHC) independent way. The MHC independence makes CARs applicable for patients independent of their Human leukocyte antigen (HLA) profile; however, the dependence on surface antigens limits the set of targets, as only approximately 20% of all cellular proteins are surface-expressed (Bausch-Fluck et al., 2018; Fagerberg, Jonasson, von Heijne, Uhlen, & Berglund, 2010; Uhlen et al., 2015). CAR T cells have demonstrated remarkable clinical results, especially for B-cell malignancies, and all clinically approved CARs recognize either CD19 or B-cell maturation antigen (BCMA) (Bonini et al., 2023). B-cell-targeted CARs have significantly advanced the field of adoptive T-cell transfer but also have the fortune of targeting a particularly favorable differentiation antigen selectively expressed on B cells: hypogammaglobulinemia and B-cell aplasia resulting from targeting all CD19- or BCMA-bearing B cells are clinically manageable with immunoglobulin replacement therapy (Cappell & Kochenderfer, 2023). This is not the case for most other human tissues from which tumors can arise, necessitating more tumor-specific targets, which are currently being investigated (Kampouri, Walti, Gauthier, & Hill, 2022; Labanieh & Mackall, 2023).

Transgenic TCRs, just like endogenous αβ-TCRs, recognize peptide fragments derived from proteins from all cellular compartments presented on MHC (in humans, HLA class 1-A/-B/-C or HLA class 2-DR/-DP/-DQ). This allows TCRs to target a broader spectrum of antigens, for example, in solid tumors lacking a defined surface marker (Baulu, Gardet, Chuvin, & Depil, 2023; Harris & Kranz, 2016). Conversely, the dependence on the highly variable HLA molecules makes a given tumor-reactive TCR only applicable to patients with the respective HLA isotype. Therefore, for therapeutic applications, either identified tumor-reactive TCRs can be used for a small group of suitable patients, or personalized TCRs must be identified that are specific for each individual patient. The individualized approach requires significant technical effort, both in the identification of suitable antigens and TCRs and in T cell engineering with personalized transgenes (Krackhardt et al., 2018). However, it makes it possible to target tumor neoantigens (Bassani-Sternberg et al., 2016; Stronen et al., 2016). These are modified peptide fragments that arise from mutations or other alterations in protein expression in cancer cells. Tumor

neoantigens are highly specific and are recognized as foreign by the immune system, thus posing an extremely attractive target for T-cell-based immunotherapies (Schumacher, Scheper, & Kvistborg, 2019). While TCR T cell therapies lag behind CAR T cells in their clinical translation, they hold enormous therapeutic potential.

1.3 Viral gene transfer systems and their disadvantages

At the time this project started in 2017, the most commonly used way to engineer T cells, both preclinically and clinically, was the usage of gamma-retroviral or lentiviral vectors or non-viral vectors such as transposons (Clauss et al., 2018; Deniger et al., 2016; Morgan et al., 2006; Peng et al., 2009; Rapoport et al., 2015; Robbins et al., 2011; Rosenberg & Restifo, 2015). These vectors integrate into the genome of T cells semi-randomly, with different preferences for different genomic locations depending on the vector (Poletti & Mavilio, 2018; Tipanee, VandenDriessche, & Chuah, 2017). Viral gene-transfer methods are well-established, efficient, and can be scaled up for clinical use, but have a few notable disadvantages.

Due to their semi-random integration pattern, they harbor the potential risk of insertional mutagenesis (Hacein-Bey-Abina et al., 2003). The transgene includes a strong exogenous promoter and could disrupt a tumor suppressor gene's function by integrating into its gene locus or upregulate a proto-oncogene by enhancing its expression with the exogenous promoter. Additionally, the number of integrated transgenes, the Vector-copy number (VCN), follows a Poisson distribution, making the produced cell product inherently diverse. Furthermore, semi-randomly integrated transgenes will be subjected to varying degrees of local chromatin dynamics, such as regional silencing. Both these factors drive the cell-to-cell variability of the produced T-cell product (Müller et al., 2021).

When transferring a transgene TCR to T cells, the two chains of the transgenic TCR are added to the two chains of the endogenous TCR (Bendle et al., 2010; van Loenen et al., 2010) **(Figure 1)**. The introduced chains must compete with the endogenous ones for CD3 binding and thus surface expression (Ahmadi et al., 2011). This effect prevents some "weak" TCRs from being sufficiently surface-expressed. Furthermore, the four chains within the T cell can form mispaired TCRs, consisting of one endogenous and one exogenous chain, with new, potentially

dangerous specificities. In a mouse model, lethal autoimmunity due to mispaired TCRs has been observed (Bendle et al., 2010). Several engineering strategies have been deployed to reduce these problems. The expression of the introduced TCR was improved by codon optimization of the transgene or by using self-cleaving 2A elements for optimal equimolar expression of the two transgenic TCR chains (Leisegang et al., 2008; Scholten et al., 2006). The stability of the introduced TCR can be improved and mispairing reduced by exchanging the constant regions of the α- and β-chains for murine sequences, by adding a cysteine bond between the two chains, by swapping domains of the constant region, or by using single-chain TCRs (Cohen, Zhao, Zheng, Rosenberg, & Morgan, 2006; Govers, Sebestyen, Coccoris, Willemsen, & Debets, 2010; Knies et al., 2016; Kuball et al., 2007). Lastly, competition with the endogenous TCR can be reduced by disrupting its gene loci with nucleases or by reducing its expression using Small interfering RNA (siRNA) (Clauss et al., 2018; Legut, Dolton, Mian, Ottmann, & Sewell, 2018; Provasi et al., 2012).

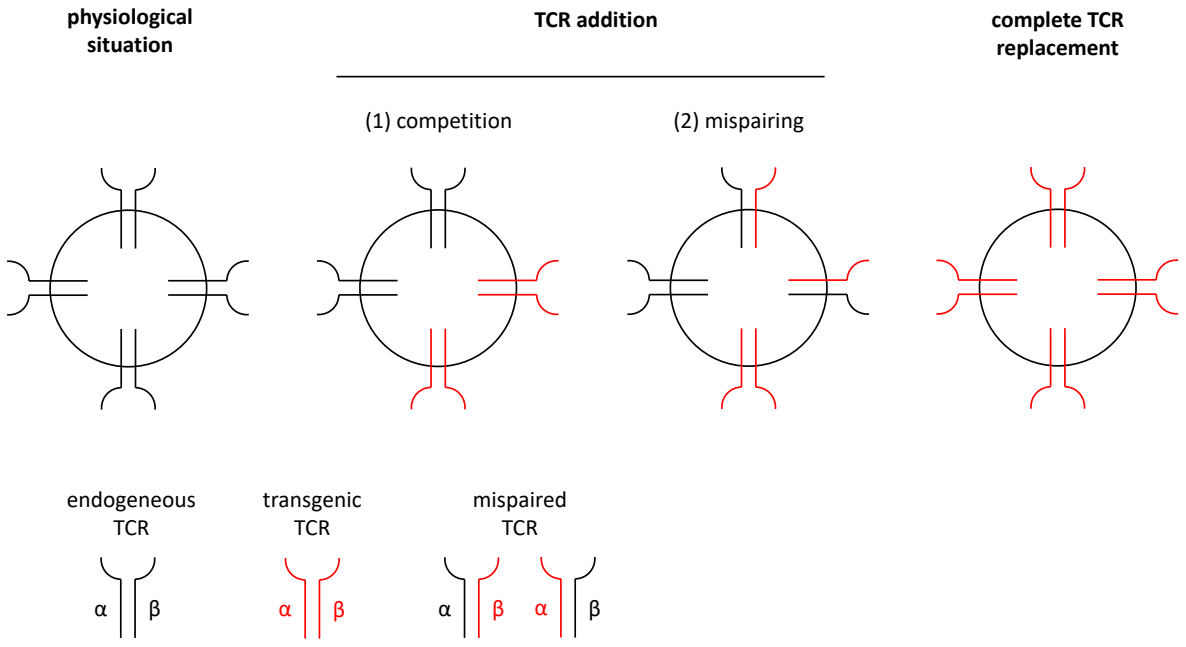

Figure 1: Competition and mispairing as a consequence of expressing two different TCRs in one T cell

1.4 T-cell editing

In addition to the introduction of large transgenes, the targeted disruption of genes represents a second pillar of T-cell engineering. Endonucleases coupled with protein-based sequence-recognition domains, such as Transcription Activator-like Effector Nucleases (TALENs), Zinc finger nucleases (ZFNs), or meganucleases, have been used to disrupt genes within T cells (Berdien, Mock, Atanackovic, & Fehse, 2014; Delhove & Qasim, 2017; Osborn et al., 2016; Provasi et al., 2012). A pioneering study by Provasi et al. (2012) demonstrated that the targeted disruption of the endogenous TCR α- and β-chain genes prior to lentiviral transduction with a tumor-reactive TCR leads to high expression of the transgenic TCR, superior antigen recognition, and diminished mispairing-induced off-target activity. However, since the sequence recognition depends on engineered protein domains, TALENs, ZFNs, and meganucleases need a lot of development effort for every new target, severely limiting their applicability.

The discovery of the Ribonucleic acid (RNA) guided Clustered Regularly Interspaced Short Palindromic Repeats (CRISPR)-Cas9 system, however, provided researchers with a versatile tool that can quickly be adapted to target a gene of interest and that can effectively be used in T cells (Bernard, Landmann, Jeker, & Schumann, 2022). Initially discovered as an adaptive immune defense against viral infections in bacteria, it was quickly developed as a genome-editing system in eukaryotic cells (Knott & Doudna, 2018; J. Y. Wang & Doudna, 2023). The power of CRISPR-Cas9 lies in its versatility: by simply exchanging the easy-to-produce guideRNA, scientists can target a different region in the genome. CRISPR associated protein 9 (Cas9) is a Deoxyribonucleic acid (DNA) endonuclease that binds an RNA-duplex consisting of a CRISPR RNA (crRNA) and a Trans-activating crRNA (tracrRNA), forming a Cas9 Ribonucleoprotein (RNP). The sequence of the crRNA defines the target location. By fusing the crRNA and tracrRNA into one single-guideRNA (sgRNA), a two-component system can be created (Jinek, Chylinski, Fonfara, Hauer, Doudna, & Charpentier, 2012). Equipped with the crRNA:tracrRNA duplex, Cas9 can bind to double-stranded DNA (dsDNA) complementary to the RNA targeting sequence if a particular DNA motif – the Protospacer adjacent motif (PAM) – is present. This “switches on” and activates the endonuclease function of Cas9, and a double-strand break (DSB) is induced (Bernard et al., 2022; Knott & Doudna, 2018). This newly generated DSB is left for the cell to repair.

Depending on the cell-cycle phase, cells repair DSB with different DNA repair pathways (Scully, Panday, Elango, & Willis, 2019; Takata et al., 1998). The most commonly used pathway active throughout the cell cycle is Nonhomologous end joining (NHEJ), an error-prone repair pathway that reconnects the two DNA ends at the cost of inducing insertions or deletions (indels). This can be used to knock out a specific gene. The introduced indels can lead to a frameshift of the open reading frame, the formation of a premature stop codon, or an altered base sequence. This leads to nonsense-mediated Messenger RNA (mRNA) decay (i.e. degradation of mRNA that does not pass an internal quality check), truncated, or mutated proteins, and thus disruption of the protein function (Popp & Maquat, 2016). During S and G2 phase, Homology-directed repair (HDR), a more precise DNA repair pathway, is active. HDR repairs the DSB based on the sequence information of a homologous chromatid. Cells can be "tricked" into introducing a transgene into the desired genomic locus by supplying an exogenous HDR template with a transgene framed by two homology arms. Other DSB repair pathways, such as the Fanconi anemia repair pathway (FA) or Microhomology-mediated end joining (MMEJ), are less prevalent, and their targetability for DNA editing is less well understood (Bernard et al., 2022).

CRISPR-Cas9 is an efficient and versatile tool to induce genetic knock-outs and knock-ins in primary human T cells (Knipping et al., 2017; Osborn et al., 2016; Schumann et al., 2015; Seki & Rutz, 2018). Moreover, the knock-in of relatively large CAR transgenes has been achieved in primary human T cells using CRISPR-Cas9 or other nucleases (Eyquem et al., 2017; Hale et al., 2017; MacLeod et al., 2017). By electroporating Cas9 mRNA and guideRNA into primary human T cells and subsequently delivering an HDR template by Adeno-associated virus serotype 6 (AAV6) encoding the CAR construct, Eyquem et al. (2017) successfully targeted the construct to the T Cell Receptor Alpha Constant (*TRAC*) locus, thereby simultaneously disrupting the endogenous TCR α-chain expression. They designed it with a promoter-trap mechanism (further explained in Results) that captures the endogenous transcription and places the construct under the gene regulatory control of the *TRAC* locus. These CAR knock-in T cells showed superior tumor control and reduced T cell exhaustion in a xenograft tumor model, which the authors attributed to reduced tonic signaling due to the transcriptional dynamic of the endogenous locus.

1.5 Aim of this study

Adoptive T cell transfer with TCR transgenic T cells holds enormous therapeutic potential. With the advent of CRISPR-Cas9 as a versatile and efficient gene editing technology, the knock-in of large transgene constructs, such as CARs, became possible.

This study aims to (1) assess if CRISPR-Cas9 and AAV6 enable the targeted integration of a tumor-reactive TCR into the *TRAC* locus, thus placing it under transcriptional control of the endogenous gene regulatory network, and (2) if this knock-in leads to the replacement of the surface-expressed TCRs by the inserted tumor-reactive TCR. We, furthermore, (3) test the *in vitro* tumor cell recognition, cytotoxicity, and Interferon gamma (IFN-γ) secretion and (4) *in vivo* migration into the tumor and tumor control, all compared to retrovirally transduced T cells.

The findings from this study help judge whether a targeted integration approach could replace semi-integrating viral transduction of T cells for future therapeutic applications.

2. Materials

2.1 Technical Equipment

Table 1: Technical Equipment

Device	Manufacturer
-20°C Freezer	Liebherr-International, Bulle, Switzerland
-80°C Freezer	Buchner Labortechnik, Pfaffenhofen, Germany
Analytical balance 440-35N	Denver Instrument, Göttingen, Germany
Analytical balance SI-64	Denver Instrument, Göttingen, Germany
AT-2 slidescanner	Leica Biosytems, Wetzlar, Germany
Autoclave Systec V95	Systec, Linden, Germany
Axiovert 40C microscope	Carl Zeiss Microscopy, Oberkochen, Germany
BD LSR II	BD Biosciences, Franklin Lakes, USA
BioDocAnalyze Gel documentation system	Biometra, Göttingen, Germany
Biometra T professional gradient Thermocycler	Biometra, Göttingen, Germany
Biometra T professional gradient Thermocycler	Biometra, Göttingen, Germany
BX53 stereomicroscope	Olympus, Shinjuku, Japan
Centrifuge 5417R	Eppendorf, Hamburg, Germany
Centrifuge 5810R	Eppendorf, Hamburg, Germany
Centrifuge J2-HS	Beckman Coulter, Brea, USA
Compact M Horizontal Gel Electrophoresis Apparatus	Biometra, Göttingen, Germany
CytoFlex	Beckman Coulter, Brea, USA
DynaMagTM-2 Magnet	Invitrogen Dynal AS, Oslo, Norway
Elelctrophoresis Apparatus i-Mupid	Cosmo Bio, Tokyo, Japan
Incubator BBD 6220	Heraeus Holding, Hanau, Germany
Incubator CB 150	BINDER, Tuttlingen, Germany
Laminar flow HERAsafe KS 15	Heraeus Holding, Hanau, Germany
Leica ASP300S Fully Enclosed Tissue Processor	Leica Biosytems, Wetzlar, Germany
MACS MultiStand	Miltenyi Biotec, Bergisch Gladbach, Germany
Micro scales Balance summit	Denver Instrument, Göttingen, Germany
Microm HM355S Rotary Microtome	Thermo Fisher scientific, Waltham, USA
NALGENE Cryo 1°C Freezing Container	Thermo Fisher scientific, Waltham, USA
NanoDrop ND-100	Peqlab Biotechnologie, Erlangen, Germany
NanoDrop Spectrophotometer ND1000	PeqLab / VWR International, Darmstadt, Germany
Neon NxT Electroporation System	Invitrogen, Carlsbad, USA
Neubauer improved counting chamber	Karl Hecht, Sondheim/Röhn, Deutschland
Pipetboy/Pipetgirl INTEGRA	Biosciences, Fernwald, Germany
Pipets	Eppendorf, Hamburg, Germany
Precision balance 440	KERN & SOHN, Balingen, Germany
Qubit 2.0 fluorometer	Thermo Fisher scientific, Waltham, USA

QX200 ddPCR system	Bio-Rad Laboratories, Feldkirchen, Germany
QX200 droplet reader	Bio-Rad Laboratories, Feldkirchen, Germany
Separator MidiMACS TM	Miltenyi Biotec, Bergisch Gladbach, Germany
StepOnePlus Real-Time PCR System	Thermo Fisher scientific, Waltham, USA
SunriseTM absorbance reader	Tecan Group Ltd., Männedorf, Switzerland
Thermomixer Compact	Eppendorf, Hamburg, Germany
VENTANA BenchMark XT automated stainer	Roche, Basel, Switzerland
VENTANA ultraVIEW DAB Detection kit	Roche, Basel, Switzerland
VICTOR Multilabel Plate Reader	PerkinElmer, Waltham, USA
Vortex-Genie 2	Scientific Industries, Bohemia, New York, USA
Waterbath	Memmert, Schwabach, Germany
Waterbath WNB	Memmert, Schwabach, Germany
Ziegra Ice machine	ZIEGRA Eismaschinen, Isernhagen, Germany

2.2 Consumables

Table 2: Consumables

Consumable	**Company**
Amicon Ultra-15 Centrifugal Filter Units	Merck, Darmstadt, Germany
Cell culture flask (T25, T75, T175)	Greiner Bio-One, Frickenhausen, Germany
Cell scraper	TPP Techno Plastic products, Trasadingen, Switzerland
CyroPure tubes	Sarstedt AG & Co., Nümbrecht, Germany
ddPCR 96-well plates	Bio-Rad Laboratories, Feldkirchen, Germany
Econopac columns	Bio-Rad Laboratories, Feldkirchen, Germany
Falcons (15ml, 50 ml)	BD Biosciences, Franklin Lakes, USA
Gloves Dermatril P	KCL, Eichenzell, Germany
MACS cell separation Columns (LD, LS, MS)	Miltenyi Biotec, Bergisch Gladbach, Germany
Microtubes (1.2ml)	Alpha laboratories, Hampshire, UK
neoScrew Micro tubes 1.5ml	neoLab Migge, Heidelberg, Germany
PCR reaction tubes (0.5 ml)	VWR International, Darmstadt, Germany
Petri dishes	Greiner Bio-One, Frickenhausen, Germany
qPCR seal	4titude Ltd., Surrey, UK
Reaction tubes (0.5µl)	Peqlab Biotechnologie, Erlangen, Germany
Sealing foil (ELISA)	Alpha Laboratories, Hampshire, UK
Sepharose G100 SF resins	Sigma-Aldrich, St. Louis, USA
Syringe filter (0,22µm and 0.45µm)	TPP Techno Plastic products, Trasadingen, Switzerland
Tissue culture-treated plates (48-well)	BD Biosciences, Franklin Lakes, USA
Tissue culture-treated plates (6-/12-/24- well, round/flat bottom 96-well)	TPP Techno Plastic products, Trasadingen, Switzerland

2.3 Mouse model

Table 3: Mouse model

Mouse line	Description	Source
NOD.CG-Prkdc^{scid} IL2rgtm^{1Wjl}/SzJ	NSG	Jackson Laboratory (Bar Harbor, Maine, USA)

2.4 Cell lines

Table 4: Cell lines

Cell line	Description	Source
ML-2	AML cell line	The Cabri consortium
293Vec-RD114	retroviral packaging cell line	BioVec Pharma, Québec, Canada
U293	AAV packaging cell line	Lab of Prof. Dr. med. Christian Kupatt-Jeremias (MRI/TUM)

2.5 Reagents and chemicals

Table 5: Reagents and chemicals

Reagent	Manufacturer
100 bp DNA Ladder	Thermo Fisher scientific, Waltham, USA
7-Aminoactinomycine D (7-AAD)	Merck, Darmstadt, Germany
Agarose standard	Roth, Karlsruhe, Germany
Alt-R S.p. Cas9 Nuclease	Integrated DNA Technologies, Coralville, USA
Ampicillin	Merck, Darmstadt, Germany
Biocoll	Merck, Darmstadt, Germany
Bovine serum albumin (BSA)	Merck, Darmstadt, Germany
customized crRNAs	Integrated DNA Technologies, Coralville, USA
customized GeneArt Strings DNA Fragment	Thermo Fisher scientific, Waltham, USA
customized pimers	Sigma-Aldrich, St. Louis, USA
D-luciferin	Gold Biotechnology, Olivette, USA
ddPCR Supermix for probes	Bio-Rad Laboratories, Feldkirchen, Germany
DEPC-H2O	Thermo Fisher scientific, Waltham, USA
DMEM (Dulbecco's Modified Eagle Medium)	Thermo Fisher scientific, Waltham, USA
DMSO (Dimethylsulfoxide)	Merck, Darmstadt, Germany
EDTA (Ethylenediaminetetraacetic acid)	Invitrogen, Carlsbad, USA
Ethanol	Merck, Darmstadt, Germany
Fetal bovine serum, heat inactivated (FCS)	Invitrogen, Carlsbad, USA
Gel Loading Dye, Purple (6X)	New England Biolabs, Ipswich, USA
GeneRuler 1 kb DNA-ladder	Thermo Fisher scientific, Waltham, USA
Gentamicin	Merck, Darmstadt, Germany
HEPES (Hydroxyethylpiperazine ethane sulfonic acid)	Invitrogen, Carlsbad, USA
Human serum, heat inactivated (HS)	Technical University of Munich, Munich, Germany

Isofluran	CP Pharma, Burgendorf, Deutschland
Isopropanol	Merck, Darmstadt, Germany
Kanamycin	Merck, Darmstadt, Germany
LB Agar	Invitrogen, Carlsbad, USA
LB Broth Base	Invitrogen, Carlsbad, USA
Non-essential amino-acids	Invitrogen, Carlsbad, USA
Paraformaldehyde (PFA)	Merck, Darmstadt, Germany
PBS (Phosphate buffered saline)	Invitrogen, Carlsbad, USA
PEI Max	Polysciences, Warrington, USA
Penicilline/Streptomycin	Thermo Fisher scientific, Waltham, USA
Pertex mounting medium	VWR, Radnor, USA
Phosphatase, Alkaline from calf intestine (CIP)	Sigma-Aldrich, St. Louis, USA
Protamine sulfate	MP Biomedicals, Illkirch, France
Retronectin	Takara, Kusatsu, Japan
RNase out	Invitrogen, Carlsbad, USA
RPMI medium	Invitrogen, Carlsbad, USA
Skim milk powder	Merck, Darmstadt, Germany
SOC outgrowth medium	New England Biolabs, Ipswich, USA
Sodium chloride	Merck, Darmstadt, Germany
Sodium pyruvate	Invitrogen, Carlsbad, USA
Streptomycin	Invitrogen, Carlsbad, USA
SYBR Safe DNA Gel Stain	Thermo Fisher scientific, Waltham, USA
T4 DNA Ligase	Thermo Fisher scientific, Waltham, USA
tracrRNA	Integrated DNA Technologies, Coralville, USA
Transfection Reagent TransIT	Mirus, Madison, USA
TRIzol reagent	Thermo Fisher scientific, Waltham, USA
Trypane blue	Thermo Fisher scientific, Waltham, USA
Trypsine EDTA: 0.5%	PAA laboratories, Pasching, Austria
Tween 20	Merck, Darmstadt, Germany

2.6 Kits

Table 6: Kits

Kit	**Manufacturer**	**Use**
BD OptEIATM TMB Substrate Reagent Set	BD Biosciences, Franklin Lakes, USA	ELISA
DNA blood and tissue kit	QIAGEN, Hilden, Germany	isolation of gDNA for Homology Arm amplification
Dynabeads Untouched Human CD8 T Cells Kit	Thermo Fisher scientific, Waltham, USA	isolation of $CD8^+$ T cells from PBMCs using negative selection
Human IFN-γ ELISA Kit	BD Biosciences, Franklin Lakes, USA	ELISA
KAPA PROBE FAST qPCR Kit	PeqLab / VWR International, Darmstadt, Germany	RT-qPCR

KAPA SYBR Fast qPCR Master Mix (2X) Universal	PeqLab / VWR International, Darmstadt, Germany	RT-qPCR
KOD Hot Start DNA Polymerase kit	Merck, Darmstadt, Germany	cloning
NEB 5-alpha Competent E. coli	New England BioLabs., Frankfurt am Main, Germany	bacterial transformation of plasmids
Neon Transfection System 10 µL Kit	Invitrogen, Carlsbad, USA	T cell electroporation
NucleoBond Xtra Maxi kit for transfection-grade plasmid DNA	Macherey Nagel, Düren, Germany	isolation of DNA for cloning purposes
NucleoSpin Gel and PCR Clean-up kit	Macherey Nagel, Düren, Germany	isolation of DNA for cloning purposes
NucleoSpin Plasmid Mini kit for plasmid DNA	Macherey Nagel, Düren, Germany	isolation of DNA for cloning purposes
Venor GeM Classic kit	Minerva Biolabs, Berlin, Germany	mycoplasma testing of cell lines
Zero Blunt TOPO PCR Cloning Kit with pCR-Blunt II-TOPO Vector	Thermo Fisher scientific, Waltham, USA	cloning

2.7 Restriction Enzymes

Table 7: Restriction enzymes

Restriction enzyme	**Manufacturer**
MluI	New England BioLabs, Ipswich, USA
AscI	New England BioLabs, Ipswich, USA
SpeI	New England BioLabs, Ipswich, USA
BstEII	New England BioLabs, Ipswich, USA
BstEII-HF	New England BioLabs, Ipswich, USA
RsrII	New England BioLabs, Ipswich, USA
EcoRI	New England BioLabs, Ipswich, USA
HindIII	New England BioLabs, Ipswich, USA
HaeIII	New England BioLabs, Ipswich, USA
MseI	New England BioLabs, Ipswich, USA

2.8 Primer and Probe sequences

Table 8: Primers used for cloning

Primer	**Sequence 5' - 3'**	**Use**	**Manufacturer**
MCS_fwd	ATACGCGTGGCGCGCCGG TACCACTAGTTTAATTAAT GATCAACGCGTAT	Used to construct a multiple clonings site (MCS) to insert into pAAV(Biolabs)-CMV-GFP	Sigma-Aldrich, St. Louis, USA
MCS_rev	ATACGCGTTGATCATTAAT TAAACTAGTGGTACCGGC GCGCCACGCGTAT	Used to construct a multiple clonings site (MCS) to insert into pAAV(Biolabs)-CMV-GFP	Sigma-Aldrich, St. Louis, USA
LHA_fwd	GGCGCGCCCACTAAGGA AAAG	Amplification of the left homology arm (~900bp)	Sigma-Aldrich, St. Louis, USA
LHA_rev	ACTAGTGTCAGGGTTCTG GATATCTG	Amplification of the left homology arm (~900bp)	Sigma-Aldrich, St. Louis, USA

RHA_fwd	GGTAACCGTATACCAGCTTCGAGACTCTAAATCCAGTGACA	Amplification of the right homology arm (~900bp)	Sigma-Aldrich, St. Louis, USA
RHA_rev	CGGTCCGCAAGTAGCATTTCTTCAGAG	Amplification of the right homology arm (~900bp)	Sigma-Aldrich, St. Louis, USA
EcoRI_targeting_construct_fwd	ATATATGAATTCGGCGCGCCC	Amplify targeting construct (LHA-PT-2.5D6omc-RHA) from pAAV(Biolabs) and add EcoRI binding sites	Sigma-Aldrich, St. Louis, USA
EcoRI_targeting_construct_rev	AATAAGAATTCCGGTCCGCAAGTAG	Amplify targeting construct (LHA-PT-2.5D6omc-RHA) from pAAV(Biolabs) and add EcoRI binding sites	Sigma-Aldrich, St. Louis, USA

Table 9: Primers and probes used for ddPCR

Primer/Probe	**Sequence 5' - 3'**	**Use**	**Manufacturer**
DO-TRAC-for	CTTGTCCATCACTGGCATCT	drop-off assay, knock-out quantification	Sigma-Aldrich, St. Louis, USA
DO-TRAC-rev	CGGTGAATAGGCAGACAGAC	drop-off assay, knock-out quantification	Sigma-Aldrich, St. Louis, USA
TRAC-probe	6FAM]AGCCTGGGTTGGGGCAAAGAGGG[BHQ1]	drop-off assay, knock-out quantification	Sigma-Aldrich, St. Louis, USA
LNA-Drop-Off	/5HEX/CCCTGC+C+G+T+GTA/3IABkFQ/	drop-off assay, knock-out quantification	Integrated DNA Technologies, Coralville, USA
LHA-for	CCCCAACATGCTAATCCTCC	LHA, knock-in quantification	Sigma-Aldrich, St. Louis, USA
LHA-rev	ACAGCAGTCCCAGAGACATA	LHA, knock-in quantification	Sigma-Aldrich, St. Louis, USA
LHA-probe	[6FAM]CCCCACAGAGCCCCGCCCT[BHQ1]	LHA, knock-in quantification	Sigma-Aldrich, St. Louis, USA
RHA-for	TCAGGTGATCTACCCAC	RHA, knock-in quantification	Sigma-Aldrich, St. Louis, USA
RHA-rev	GTCTACCCTCTCATGGCCTA	RHA, knock-in quantification	Sigma-Aldrich, St. Louis, USA
RHA-probe	[HEX]CAGGGCCGGGTCACAGGGCC[BHQ1]	RHA, knock-in quantification	Sigma-Aldrich, St. Louis, USA
EIF2C1-for	CCTGCCATGTGGAAGATGAT	reference	Integrated DNA Technologies, Coralville, USA
EIF2C1-rev	GAGTGTGGTCACTGGACTTG	reference	Integrated DNA Technologies, Coralville, USA
EIF2C1-probe	/5HEX/ACCAGTCTG/ZEN/TGCGCCCTGCCA/	reference	Integrated DNA Technologies, Coralville, USA

2.9 Vectors

Table 10: Vectors

Plasmid	Description
pAAV(Wilson)-LHA-PT-2.5D6omc-RHA	ITR-bearing plasmid with targeting construct (LHA-PT-2.5D6omc-RHA) used to generate AAV, based on pAAV(Wilson)-CMV-eGFP by Prof. James Wilson (Perelman School of Medicine, University of Pennsylvania)
pAAV(Biolabs)-CMV-GFP	AAV-plasmid (Cell Biolabs)
pAAV(Wilson)-CMV-eGFP	AAV-plasmid (AG Kupatt, gifted from Prof. James Wilson, University of Pennsylvania)
MP71-2.5D6	MP71-based retroviral plasmid encoding the TCR2.5D6, under transcriptional control of a MPSV-LTR promotor. Designed by Klar et al. (2014)
helper plasmid δ F6	helper plasmid (AG Kupatt, Puresyn), for recombinant AAV production
cap-rep-plasmid	plasmid endoing "cap" and "rep" (AG Kupatt), for recombinant AAV production

2.10 GuideRNAs

Table 11: GuideRNAs

crRNA	Sequence 5' - 3'	Manufacturer
anti-*TRAC* crRNA	TCTCTCAGCTGGTACACGGC	Integrated DNA Technologies, Coralville, USA
non-targeting control crRNA	GTATTACTGATATTGGTGGG	Integrated DNA Technologies, Coralville, USA

2.11 Antibodies

Table 12: Antibodies used for flow cytometry

Antibody	Isotype	Fluorophore	Clone	Company	Dilution
anti-human TCRα/β	mouse IgG2b	PE	BW242/412	Miltenyi Biotec, Bergisch Gladbach, Germany	1:150
anti-mouse TCR β chain	armenian hamster IgG2, λ1	APC	H57-597	BD Biosciences, Franklin Lakes, USA	1:75
anti-human CD3	mouse BALB/c IgG1, κ	PE	UTCH1	BD Biosciences, Franklin Lakes, USA	1:75

Table 13: Antibodies used for immunohistochemistry

Antibody	Isotype	Clone	Company	Dilution
anti-human CD3	Rabbit IgG_1	MRQ-39	Cell Marque, Rocklin, USA	1:500

2.12 Media and buffers

Table 14: Media

Medium	Components
Freezing medium	90 % ΔFCS, 10 % DMSO
cRPMI	RPMI 1640 with phenol red, 10 % (v/v) ΔFCS, 2 mmol/l L-Glutamine, 10 mmol/l non-essential amino-acids, 1 mmol/l Sodium-Pyruvat, 100 IU/ml Penicillin/Streptomycin
cDMEM	DMEM with phenol red, 10 % (v/v) ΔFCS, 2 mmol/l L-Glutamine, 10 mmol/l non-essential amino-acids, 1 mmol/l Sodium-Pyruvat, 100 IU/ml Penicillin/Streptomycin
T cell medium	RPMI 1640 with phenol red, 5 % (v/v) ΔFCS, 5 % (v/v) ΔHS, 10 mmol/l HEPES, 16.6 µg/ml Gentamycin, 2 mmol/l L-Glutamine, 10 mmol/l non essential AS, 1 mmol/l Sodium-Pyruvat, 100 IU/ml P/S

Table 15: Buffers

Buffer	Components	Use
Coating buffer	0.1 mol/l $NaHCO_3$, 0.03 mol/l Na_2CO_3, H_2O, pH 9.5	ELISA
ΔFCS	Inactivated FCS, 20min @ 58°C	Additive for media and buffers
ΔHS	Inactivated HS, 20min @ 58°C	Additive for media and buffers
10x TAE buffer	0.4 mmol/l Tris-HCl, pH 7.8	DNA gel electrophoresis
Blocking buffer	PBS, 1% milk powder	ELISA
FACS buffer	PBS, 10% FCS	Flow cytometry
Fixation buffer	PBS, 1% PFA	Flow cytometry
Isolation buffer	PBS, 0.2 % ΔFCS, 2 mmol/l EDTA	Beads-based cell isolation
Luciferin solution	PBS, 10% FCS, 150 µg/ml D-luciferin	Luciferase-based cytotoxicity assay
RetroNectin solution	PBS, 12.5 µg/ml RetroNectin	Gammaretroviral transduction
washing buffer	PBS, 0.05% Tween-20	ELISA

2.13 Recombinant cytokines

Table 16: Recombinant cytokines

Cytokine	Manufacturer
reombinant human IL-2	PeproTech, London, UK
reombinant human IL-7	PeproTech, London, UK
reombinant human IL-15	PeproTech, London, UK

2.14 Software and web-based tools

Table 17: Software and web-based tools

Software	Use	Manufacturer/Origin
Aperio Imagescope software	histological image acquisition	Leica Biosytems, Wetzlar, Germany

Benchling	cloning management	Benchling, San Francisco, USA
BLAST	histological image acquisition	National Institutes of Health (NIH), Bethesda, USA
Endnote	Reference management	Clarivate Analytics, Philadelphia, USA
FlowJo 10	Flow Cytometry data analysis	FlowJo, LLC, Ashland, USA
GraphPad Prism 7	statistical analysis	GraphPad Software, La Jolla, USA
Microsoft Office	data analysis, presentations, manuscript	Microsoft, Redmond, USA
Primer3Plus	primer design	EMBL, Heidelberg, Germany
QuantaSoft v1.7.4	ddPCR analysis	Bio-Rad Laboratories, Feldkirchen, Germany
R programming language	ddPCR analysis	The R Project for Statistical Computing
Wellcome Sanger Institute Genome Editing (WGE) tool	gRNA design	Wellcome Sanger Institute, Hinxton, UK

3. Methods

3.1 Cell culture

3.1.1 General cell culture conditions

All cell culture was performed under biosafety level S2 working conditions according to the specifications of the local authorities. All work was done under sterile biological safety cabinets.

3.1.1.1 Counting cells

Cells were counted microscopically with a Neubauer chamber. For this, cells were diluted to a concentration at which the counting was feasible, and 1% trypan blue solution was added. This allowed the exclusion of dead cells, and only live cells were used for cell concentration determination. At least five squares were inspected for cell counting. Cell concentrations were calculated with the following formula:

$$cell\ concentration = \frac{Number\ of\ live\ counted\ cells * dilution\ factor}{number\ of\ counted\ squares} * 10^4$$

3.1.1.2 Freezing and thawing cells

For freezing, cells were first spun pelleted (5min, 500g) in a 15ml falcon. After careful aspiration of the supernatant, the supernatant was resuspended in 1ml freezing medium (Fetal calf serum (FCS) with 10% Dimethylsulfoxide (DMSO)). The suspension was transferred to a labeled cryotube and placed in a pre-cooled (4°C) cooling box. Cells were kept in a -80°C fridge for 1 day and then transferred to liquid nitrogen. For thawing, cells were placed in a 37°C water bath immediately after retrieval from the liquid nitrogen tank until the vial's content became liquid. Cells were diluted in 1ml or pre-warmed RPMI, pelleted, and resuspended in prewarmed, appropriate medium.

3.1.2 PBMC and T cell culture

3.1.2.1 PBMC isolation

Healthy donors who had given their consent according to the Helsinki Declaration and the local ethical board donated whole blood. Peripheral blood mononuclear cell (PBMCs) were

isolated using a Biocoll (Merck) density gradient. Equal volumes of Ethylenediaminetetraacetic acid (EDTA) blood samples and RMPI were mixed. 35ml of this mixture was carefully placed on 15ml of Biocoll reagent in a 50ml falcon and centrifuged for 20min at 880g with the brakes off. Carefully, the buffy coat was aspirated and washed two times with RPMI. PBMCs were resuspended at a cell concentration of ~10^6 cells/ml in T-cell medium.

3.1.2.2 $CD8^+$ T cell isolation

$CD8^+$ T cells were isolated by negative selection using the Dynabeads Untouched Human CD8 T cell Kit (Thermo Fischer Scientific) according to the manufacturer's recommendations. Briefly, approximately 10^8 cells were thawed and pelleted. The pellet is resuspended in 400µl isolation buffer. 100µl staining-antibody mix is added and carefully but thoroughly mixed. The mixture is incubated at 4°C for 5min. 300µl isolation buffer and 200µl of the resuspended beads cocktail are added. The isolation column is placed in the magnetic field and 3ml of isolation buffer is applied to the column. The cell-beads mix is applied to the column and the flowthrough – which contains the negatively selected $CD8^+$ T cells – is collected. Another 3ml of isolation buffer is added and the flowthrough is collected once more. As a negative control, the column is removed from the magnetic field and the antibody-beads-bound cells are harvested by adding another 3ml to the column and pressing the liquid with plunger through the column. Isolation purity is determined by flow cytometry.

3.1.2.3 T cell culture

T cells were kept at ~10^6 cells/ml in T-cell medium. Human Interleukin (IL)-7 and human IL-15 (both PeproTech) were added to the medium at a final concentration of 5 ng/ml each. Cells were split every 2-3 days with fresh medium and replenishment of the cytokines.

3.1.2.4 T cell activation

T cells were activated with Dynabeads Human T-Activator CD3/CD28 (Thermo Fisher Scientific) according to the manufacturer's recommendations at a bead-to-cell ratio of 1:1 in the presence of 30 IU/ml human IL-2 (PeproTech). Cells were cultured in 24-well plates for 72h at 37°C.

3.1.3 Cell line cell culture

The Acute myeloid leukemia (AML) cell line ML-2 (The Cabri consortium) was cultured in suspension in cRPMI. 293Vec-RD114 (BioVec Pharma) and U293 (Kupatt Lab) cells were kept at approximately 70% adherence in cDMEM. Cells were regularly inspected under the light microscope and split two times per week or once the medium started to turn yellow. To split adherent cells, the cell culture flask was carefully clapped till detachment was macroscopically visible, 10ml of PBS was added, and cells were pelleted and resuspended in fresh cell culture medium. All cell lines were regularly tested for mycoplasma infection (Venor GeM Classic kit).

3.2 Cloning of the targeting construct

3.2.1 General cloning strategy

For the generation of AAV6 carrying the repair template, we cloned the transgene-carrying plasmid pAAV(Wilson)-LHA-PT-2.5D6omc-RHA **(Figure 2)**. This plasmid is based on the backbone vector pAAV(Wilson)-CMV-eGFP and carries the left homology arm (LHA), the tumor-reactive TCR construct (2.5D6omc), preceded by a Peptide 2A (P2A) element serving as a promoter trap (PT) and followed by a polyA-sequence and the Right homology arm (RHA). The donor template is placed between two Inverted terminal repeat (ITR) sequences that serve as the cis-acting packaging signal during Adeno-associated Virus (AAV) production. Broadly speaking, we amplified the homology arms from genomic DNA and ordered the PT-2.5D6omc construct as GeneArt Gene String. These elements were initially cloned into the pAAV(Biolabs) backbone vector by Cell Biolabs but later transferred to a different pAAV backbone vector pAAV(Wilson) and subsequently used for AAV production **(Figure 3)**.

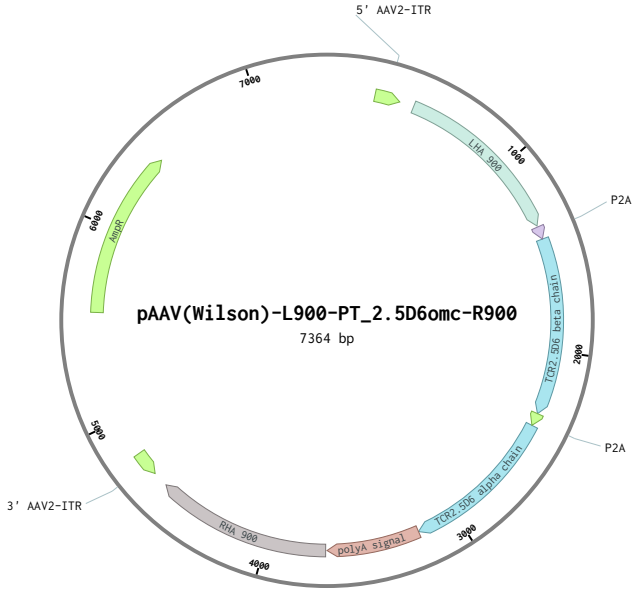

Figure 2: Plasmid map pAAV(Wilson)-LHA-PT_2.5D6omc-RHA

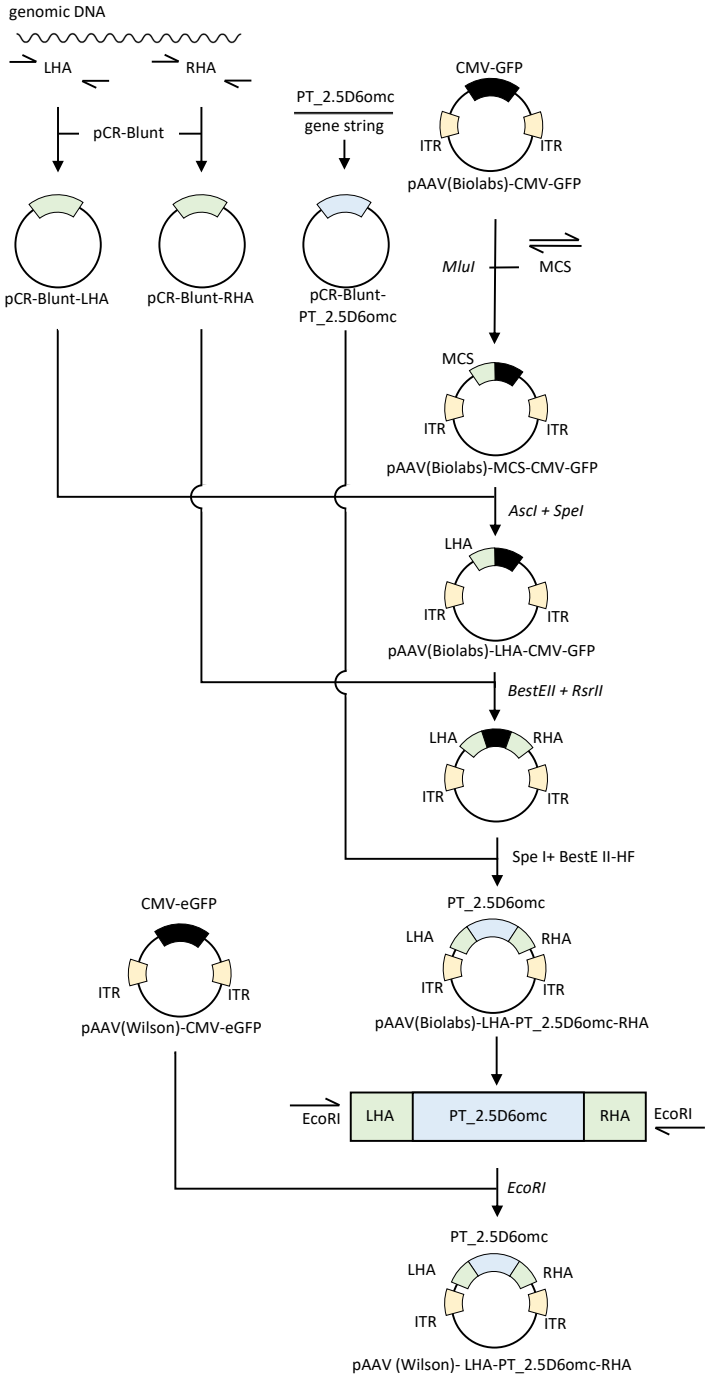

Figure 3: Overview of the cloning-strategy of pAAV(Wilson)-LHA-PT_2.5D6omc-RHA

3.2.2 Cloning of a Multiple cloning site into pAAV(Biolabs)-CMV-GFP

Initially a the vector pAAV(Biolabs)-CMV-GFP (Cell Biolabs) was used as a backbone to construct the donor template. For this, a Multiple cloning site (MCS) was generated by resuspending two complementary oligonucleotides (MCS_fwd and MCS_rev) (Sigma-Aldrich) with Diethyl pyrocarbonate (DEPC)-H2O to a concentration of 100 µM. Those were mixed equimolarly and annealed using the thermocycler conditions displayed in **Table 18** to generate

a double-strand MCS. This was subsequently inserted into pAAV(Biolabs)-CMV-GFP between the left terminal repeat and the CMV-promoter using restriction-ligation cloning with *MluI* (New England Biolabs) to generate pAAV(Biolabs)-MCS-CMV-GFP. For this, pAAV(Biolabs)-CMV-GFP and the dsDNA MCS were digested using the digestion mix and incubation conditions described in **Table 19**. The digested vector and insert were ligated using the T4 DNA Ligase (Thermo Fischer Scientific) as described in **Table 20** and were transformed into NEB 5-alpha Competent E. coli (High Efficiency; New England Biolabs) for vector amplification using the heat-shock method as recommended by the manufacturer. As a control, a ligation mix without the insert was transformed into competent E. coli. Plasmid-bearing bacteria were selected on Ampicillin-containing agar plates. Individual colonies were picked and cultured in 1ml of Ampicillin-containing bacterial culture medium at 37°C overnight, and plasmid-DNA was isolated using the NucleoSpin Plasmid Mini kit for plasmid DNA (Macherey-Nagel). The correct sequence was confirmed via Sanger-sequencing (Eurofins Genomics) and the plasmid was re-transformed into NEB 5-alpha Competent E. coli (High Efficiency) (New England Biolabs), followed by another bacterial amplification and plasmid isolation.

Table 18: Thermocycler conditions for the annealing of the MCS-oligos

Component	**Volume**	**Incubation**
MCS_fwd	5 µl	5min @ 95°C 5min @ 95°C lowering to 85°C 10min @ 85°C lowering to 25°C Hold @ 4°C
MCS_rev	5 µl	

Table 19: *MluI* restriction mixtures

Component	**Volume - Vector digestion**	**Volume - dsDNA-MCS digestion**	**Incubation**
MluI	1 µl	1 µl	1h @ 37°C 20min @ 80°C
NEB Buffer 3.1	5 µl	5 µl	
DNA	1 µl ≈ 1 µg	5 µl ≈ 500 ng	
PCR grade H2O	43 µl	39 µl	

Table 20: T4 DNA ligation mixture

Component	Volume	Incubation
Digested vector	1 µl ≈ 20 ng	Overnight @ 16°C 10min @ 65°C kept on ice until transformation
Digested insert	1 µl ≈ 10 ng	
5X T4 DNA-ligase buffer	4 µl	
T4 DNA-ligase	1 µl	
PCR grade H2O	13 µl	

3.2.3 Cloning of the Homology Arms into pAAV(Biolabs)-MCS-CMV-GFP

Genomic DNA was isolated from cultured human T cells using the DNA Blood and tissue isolation kit (Quiagen) according to the manufacturer's recommendations and resuspended in 20-50 µl DEPC-H2O. Two approximately 900 bp long homology arms flanking the expected cut site in the first Exon of the *TRAC* locus (3' and 5') were amplified from genomic DNA using the primers LHA_fwd, LHA_rev, RHA_fwd, and RHA_rev which were designed with the help of Primer3Plus (Untergasser, Nijveen, Rao, Bisseling, Geurts, & Leunissen, 2007).

To prevent re-cutting of the integrated sequence the primers LHA_rev and RHA_fwd, which amplify the regions surrounding the cut site, were silently mutated: The PAM used by *S. pyogenes* Cas9 at the targeted cut site (5'-NGG-3') which is amplified by LHA_rev and the guideRNA (gRNA) binding site downstream of the cut-site were silently mutated to prevent RNP binding and cutting, while the original amino-acid sequence was preserved. The Polymerase chain reaction (PCR) was performed using the KOD Hot Start DNA Polymerase kit (Merck) **(Table 21)**. The amplicon's size was verified on a 0.7% agarose gel (20min, 150V). The PCR products were eluted from the gel using the NucleoSpin kit (Macherey-Nagel), cloned into pCR-Blunt plasmids (Thermo Fisher Scientific) following the manufacturer's recommendations, transformed into NEB 5-alpha Competent E. coli (High Efficiency; New England Biolabs), and cultured on Kanamycin-containing plates. As described earlier individual colonies were isolated, Sanger-sequenced and the correct plasmid was re-transformed and bacterially amplified.

Table 21: PCR-amplification of the homology arms from genomic DNA

Component	**Volume**	**Incubation**
10x Buffer for KOD Hot Start DNA Polymerase	5 µl	Activation: 2min @ 95°C 40 cycles of: Denaturation: 20sec @ 95°C Annealing: 10sec @ 68°C Extension 15sec @ 70°C Hold @ 4°C
25mM MgSO4	3 µl	
dNTPs (2 mM each)	5 µl	
PCR Grade H2O	28 µl	
FWD primer (10 µM)	1.5 µl	
Rev primer (10 µM)	1.5 µl	
genomic DNA	5 µl = 100 ng	
KOD Hot Start DNA Polymerase (1.0 IU/µL)	1 µl	

First, the LHA was cloned into the MCS of pAAV(Biolabs)-MCS-CMV-GFP using restriction-ligation cloning. For the restriction, *AscI* (New England Biolabs) and *SpeI* (New England Biolabs) were used **(Table 22)**. After restriction, 10 µl 6x NEB Loading Dye was added (New England Biolabs) and the digestion product was confirmed on a 0.7% agarose gel (20min, 150V), from which the band of the expected size was isolated using the Nucleospin Gel and PCR Clean-up kit (Macherey-Nagel). This was followed by followed by DNA ligation **(Table 23)**, transformation, sequencing, retransformation, and plasmid isolation as described earlier.

Table 22: *AscI* and *SpeI* restriction mixtures

Component	**Volume –** pAAV(Biolabs)-MCS-CMV-GFP	**Volume -** pCR-Blunt-LHA	**Incubation**
AscI	1 µl	1 µl	1h @ 37°C
SpeI	1 µl	1 µl	
10x CutSmart Buffer	5 µl	5 µl	
DNA	1 µl ≈ 1 µg	10 µl ≈ 1 µg	
PCR grade H2O	42 µl	33 µl	

Table 23: T4 DNA ligation mixture to generate pAAV(Biolabs)-LHA-CMV-GFP and pAAV(Biolabs)-LHA-CMV-GFP-RHA

Component	**Volume**	**Incubation**
Digested vector	2 µl ≈ 110 ng	10min @ Room Temperature 10min @ 65°C kept on ice until transformation
Digested insert	4 µl ≈ 110 ng	
5X T4 DNA-ligase buffer	4 µl	
T4 DNA-ligase	1 µl	
PCR grade H2O	9 µl	

Subsequently, the RHA was cloned downstream of the CMV-GFP expression cassette via restriction-ligation cloning with *BstEII* (New England Biolabs) and *RsrII* (New England Biolabs) **(Table 24)** and the same steps followed as described for the LHA.

Table 24: Two-step restriction digestion with *RsrII* and *BstEII*

Component	**Volume –** pAAV(Biolabs)-LHA-CMV-GFP	**Volume -** pCR-Blunt-RHA	**Incubation**
RsrII	1 µl	1 µl	1h @ 37°C
10x CutSmart Buffer	5 µl	5 µl	
DNA	10 µl ≈ 1 µg	10 µl ≈ 1 µg	
PCR grade H2O	34 µl	34 µl	
NaCl solution (292,2 mg/ml)	1 µl	1 µl	15min @ 60°C
BstEII	1 µl	1 µl	

3.2.4 Cloning of the targeting construct PT-2.5D6omc into pAAV(Biolabs)-LHA-CMV-GFP-RHA

The target construct was custom-made as Invitrogen GeneArt Strings DNA Fragment (Thermo Fischer Scientific). The construct contains the codon-optimized (o) TCR α- and TCR β-chain of the tumor-reactive TCR2.5D6omc with murinized constant (m) regions in which an additional cysteine-bridge (c) between the α- and β-chain was introduced for increased stability, surface-expression and reduced mispairing (Kuball et al., 2007). TCR2.5D6omc recognizes a myeloperoxidase-derived peptide-epitope when presented on HLA-B7 (Klar et al., 2014). The TCR-construct is preceded by a “self-cleaving” P2A element which serves as a promoter-trap (PT) that places the transgene under the endogenous transcriptional control when integrated in-frame in the first *TRAC* exon (Eyquem et al., 2017). Furthermore, the two TCR chains are

also separated by a P2A element to enable bicistronic, equimolar protein-translation from the same mRNA molecule (J. H. Kim et al., 2011) **(Figure 2)**.

The GeneArt Strings DNA Fragment was cloned into a pCR-Blunt plasmid (Thermo Fisher Scientific), transformed into NEB 5-alpha Competent E. coli (High Efficiency; New England Biolabs) and individual colonies were picked from Kanamycin containing agar plates. The correct sequence was confirmed by Sanger-sequencing (Eurofins Genomics), retransformed into competent E. coli and isolated using the NucleoBond Xtra Maxi kit for transfection-grade plasmid DNA (Macherey Nagel). The targeting construct was cloned between the two homology arms in pAAV(Biolabs)-LHA-CMV-GFP-RHA to replace the CMV-GFP expression cassette using restriction-ligation cloning and to generate pAAV(Biolabs)-LHA-PT-2.5D6omc-RHA. For this, the restriction enzymes *SpeI* and *BstEII-HF* were used **(Table 25)**, followed by gel isolation (0.7% agarose gel, 20min, 150V) of the correct fragments, ligation **(Table 26)**, transformation, isolation, sequencing, and re-transformation as described earlier. Finally, the plasmid was isolated using the NucleoBond Xtra Maxi kit for transfection-grade plasmid DNA (Macherey Nagel).

Table 25: Restriction digestion with *SpeI* and *BstEII-HF*

Component	**Volume –** pAAV(Biolabs)-LHA-CMV-GFP-RHA	**Volume -** pCR-Blunt-PT-2.5D6omc	**Incubation**
SpeI	1 µl	1 µl	30min @ 37°C
BstEII-HF	1 µl	1 µl	
10x CutSmart Buffer	5 µl	5 µl	
DNA	10 µl ≈ 1 µg	10 µl ≈ 1 µg	
PCR grade H2O	33 µl	33 µl	

Table 26: T4 DNA ligation mixture to generate pAAV(Biolabs)-LHA-PT-2.5D6omc-RHA

Component	**Volume**	**Incubation**
Digested vector	0.5 µl	Overnight @ 16°C 10min @ 65°C kept on ice until transformation
Digested insert	4 µl	
5X T4 DNA-ligase buffer	4 µl	
T4 DNA-ligase	1 µl	
PCR grade H2O	10.5 µl	

3.2.5 Cloning the targeting construct into pAAV(Wilson)-CMV-eGFP to generate pAAV(Wilson)-LHA-PT-2.5D6omc-RHA

We transferred the targeting construct (LHA-PT-2.5D6omc-RHA) to the backbone vector pAAV(Wilson)-CMV-eGFP to generate pAAV(Wilson)-LHA-PT-2.5D6omc-RHA, as this vector has previously been shown to generate high-titers of AAV6 (Ziegler et al., 2017). The vector bears two ITRs derived from Adeno-associated virus serotype 2 (AAV2) which serve as a *cis*-acting packaging signal between which the targeting construct was placed. pAAV(Wilson)-CMV-eGFP was kindly supplied by the research group of Prof. Dr. med. Christian Kupatt-Jeremias (Klinik und Poliklinik für Innere Medizin I, Klinikum Rechts der Isar, TUM) and was originally a gift from Prof. James Wilson (Perelman School of Medicine, University of Pennsylvania).

To transfer the targeting construct including both homology arms from pAAV(Biolabs) to pAAV(Wilson), it was first amplified with PCR-primers bearing an *EcoRI* binding site (EcoRI_targeting_construct_fwd, EcoRI_targeting_construct_rev) **(Table 27)** and subsequently cloned into pAAV(Wilson) using restriction-ligation cloning. For this, the backbone vector pAAV(Wilson)-CMV-eGFP was digested using *EcoRI* and subsequently treated with Calf Intestine Alkaline Phosphatase (CIP, Sigma Aldrich) to remove the remaining phosphate rests at the cut sites, thus reducing rejoining of the backbone vector without the insert during ligation **(Table 28)**. The PCR amplicon was digested with *EcoRI* **(Table 28)** without the use of CIP. The digestion products were run on a 0.7% agarose gel (20min, 150V), and eluted from the gel using the NucleoSpin Gel and PCR Clean-up kit (Macherey-Nagel). Subsequently, they were ligated using the T4 DNA ligase, transformed into competent bacteria and isolated using the NucleoBond Xtra Maxi kit for transfection-grade plasmid DNA (Macherey Nagel), all as described earlier. The final construct was confirmed using Sanger-sequencing.

Table 27: PCR-Amplification of the targeting construct from pAAV(Biolabs)-LHA-PT-2.5D6omc-RHA

Component	**Volume**	**Incubation**
10x Buffer for KOD Hot Start DNA Polymerase	5 µl	Activation: 2min @ 95°C 40 cycles of: Denaturation: 20sec @ 95°C Annealing: 10sec @ 60°C Extension 80sec @ 70°C Hold @ 4°C
25mM MgSO4	3 µl	
dNTPs (2 mM each)	5 µl	
PCR Grade H2O	28 µl	
Fwd primer (10 µM)	1.5 µl	
Rev primer (10 µM)	1.5 µl	
Plasmid DNA	5 µl = 100 ng	
KOD Hot Start DNA Polymerase (1.0 IU/µL)	1 µl	

Table 28: Restriction digestion with *EcoRI* with and without CIP

Component	**Volume –** pAAV(Wilson)-CMV-eGFP	**Volume -** PCR amplicon of targeting construct	**Incubation**
EcoRI	1 µl	1 µl	3h @ 37°C
10x EcoRI Buffer	2 µl	2 µl	
DNA	1 µl	2 µl	
PCR grade H2O	15 µl	15 µl	
CIP (10 IU/µl)	1 µl	-	30min @ 37°C

3.3 Genetic modification techniques

3.3.1 CRISPR-Cas9

3.3.1.1 Cas9 Ribonucleoprotein Production

We designed a gRNA targeting the first exon of the *TRAC* locus using the Wellcome Sanger Institute Genome Editing (WGE) tool (Hodgkins et al., 2015). The targeted cut-site is located upstream of the transmembrane domain of the endogenous TCR α-chain to prevent the remnant peptide fragment left after successful editing to bind the endogenous β-chain and to localize to the cell membrane (Eyquem et al., 2017). As a negative control, a previously published non-targeting gRNA was chosen (Doench et al., 2016). gRNAs were synthesized as crRNAs by Integrated DNA Technologies. To generate the RNPs, the gRNA is assembled from crRNA and tracrRNA according to the manufacturer's recommendations. Briefly, crRNA and tracrRNA are each resuspended in IDTE Buffer to a final concentration of 200 µM. Those are mixed equimolarly to a final concentration of 44 µM and carefully resuspended. The mixture

is heated to 95°C for 5 min and left to cool to room temperature for 15 min to allow hybridization of the crRNA:tracrRNA-duplex. For RNP formation, Alt-R S.p. Cas9 Nuclease (Integrated DNA Technologies) was resuspended in Resuspension buffer R from the Neon Transfection System 10 µL Kit (Invitrogen) to a final concentration of 36 µM. Equal volumes of crRNA:tracrRNA-duplex and the diluted Alt-R S.p. Cas9 Nuclease are mixed, gently resuspended, and incubated for 20 min at room temperature. The generated RNP mixture is stored at 4°C until use.

3.3.1.2 Gene editing of primary human T cells

Before gene editing, primary human T cells were activated for 72h and the Human T-Activator CD3/CD28 Dynabeads were removed before electroporation. Per electroporation condition, 1 million T cells were washed in prewarmed Dulbecco's phosphate-buffered saline (DPBS), spun down (500g, 5min, room temperature), and resuspended in 11 µl buffer R of the Neon Transfection System Kit (Invitrogen) and kept on ice. Per condition, 1 µl of RNP mixture was added and carefully resuspended. 10 µl of the mixture was carefully taken up with the 10 µl Neon electroporation pipette without taking up any bubbles and electroporated at 1600V with 3 pulses of 10ms each with a Neon NxT Electroporation System (Invitrogen). After electroporation, the cells were transferred into 1 ml of prewarmed T cell medium in a 24-well plate. For TCR knock-in AAV6 containing the HDR template encoding TCR2.5D6 was added at a Multiplicity of infection (MOI) of 10^6 immediately afterwards. For TCR knock-out PBS was added as control.

3.3.2 Recombinant Adeno-associated Virus serotype 6 (AAV6) production

AAV6 production was kindly performed by Anja Wolf (research group of Prof. Dr. med. Christian Kupatt-Jeremias, Klinik und Poliklinik für Innere Medizin I, Klinikum Rechts der Isar, TUM) following a previously described protocol (Ziegler et al., 2017). For the production of replication-incompetent AAVs of serotype 6 particles the packaging cell line U293 is transfected with three plasmids: a plasmid encoding the “cap” sequence of AAV6 and the “rep” sequence of AAV2, helper plasmid δ F6 (Puresyn), and the plasmid pAAV(Wilson)-LHA-PT-2.5D6omc-RHA that bears genetic cargo of the AAV. All three plasmids are transfected into U293 cells using PEI Max (Polysciences). After 72h, AAV6 can be isolated by harvesting the

cells and preforming iodixanol-gradient centrifugation. For further purification, Sepharose G100 SF resins (Sigma-Aldrich) in Econopac columns (Bio-Rad Laboratories) are used for flow size exclusion following a protocol kindly provided by the Salk Institute for Biological Studies. Concentration of the virus in DPBS was done using Amicon Ultra-15 Centrifugal Filter Units (Merck). The viral titer was determined by Real-time quantitative polymerase chain reaction (qPCR) following a previously described protocol and the virus was stored at 4°C until use (Aurnhammer et al., 2012).

3.3.3 Retroviral gene transfer

3.3.3.1 Production of retroviral particles

The production of replication-incompetent retroviral particles for gene transfer follows a previously described protocol (Liang et al., 2010). The packaging cell line 293Vec-RD114 (BioVec Pharma), which stably expresses the genes “gag” and “pol”, is transfected with the retroviral vector plasmid pMP71-2.5D5 (Klar et al., 2014). For this, 2.5 x 10^5 293Vec-RD114 cells were resuspended in cDMEM and plated in 6-well plates. The next day, confluence should be around 60%. For transfection, 9 µl TransIT reagent (Mirus Bio LLC) is thoroughly mixed with 200 µl serum-free Dulbecco's Modified Eagle Medium (DMEM) and incubated 20min at room temperature. Next, 1µg of pMP71-2.5D5 vector plasmid DNA is added, mixed, and incubated for another 30min at room temperature. The transfection mixture is carefully dripped on the 293Vec-RD114 cells. On days 1 and 2 after transfection half of the supernatant containing the retroviral particles can be harvested and filtered with a 0.45 µm syringe filter.

3.3.3.1 Retroviral transduction of primary human T cells

First, a 24-well plate is prepared by coating it in 400 µl retronectin solution (PBS, 12.5 µg/ml RetroNectin), incubating it overnight at 4°C, and blocking the plates with 500 µl 2% Bovine serum albumin (BSA)/PBS solution, incubating at 37°C for 30min. Subsequently, the plates are washed 2 times with DPBS supplemented with 2.5% v/v Hydroxyethylpiperazine ethane sulfonic acid (HEPES). 10^6 activated primary human $CD8^+$ T cells are resuspended in 1ml T cell medium supplemented with 200 IU/ml hIL-2, 2% HEPES, and 8 µg/ml protamine sulfate and added to the prepared 24-well plates. 1 ml of filtered transfection-supernatant containing the retroviral particles is added and the plates are centrifuged for 90min at 820g without breaks.

After 1 day of incubation at 37°C, T cells are split 1:2 and the same transduction procedure is repeated. The next day, the supernatant is removed and T cells are transferred to standard T cell culture conditions. Retrovirally transduced T cells are cultured and expanded for 5 days before being analyzed by flow cytometry and being used for functional assays.

3.4 Flow cytometry

Approximately 10^5 cells were washed in Fluorescence Activated Cell Sorting (FACS) buffer (see media and buffers) in plates. For this, cells were pelleted at 500g for 5 min and the supernatant was flicked out. For blocking, cells were gently resuspended in 50 µl human serum and kept on ice for 10 min. Cells were washed again with FACS buffer, pelleted, and resuspended in 50 µl FACS buffer with the respective antibodies and 5 ng/µl 7-AAD for live-dead exclusion. Cells were stained on ice for 20 min and subsequently washed again. For fixation, cells were pelleted and resuspended in 1% Paraformaldehyde (PFA) fixation buffer and stored on ice in the dark until measurement. Cells were analyzed on an LSRII Flow Cytometer (BD) or CytoFlex (Beckman Coulter) and data analysis was done using FlowJo10 (FlowJo LLC).

3.5 Digital-droplet PCR (ddPCR)

The primers and probes for the specific digital droplet PCR assays were designed by the author, ddPCR experiments and the subsequent data analysis were performed and described by Silvia Thoene, Christof Winter, and Ramona Secci. The following description of these methods has previously been published (Albers et al., 2019).

3.5.1 Experimental procedure of ddPCR

Genomic DNA was isolated from the cells with the DNeasy Blood & Tissue kit (QIAGEN), following the manufacturer's instructions. DNA was quantified using a Qubit 2.0 fluorometer (Thermo Fisher Scientific). ddPCR analysis was performed on a QX200 ddPCR system with automatic droplet generation (Bio-Rad Laboratories). Reactions were carried out in ddPCR 96-well plates (#12001925; Bio- Rad Laboratories) and were performed in duplicate in a reaction volume of 21 µl using the ddPCR Supermix for probes (no UTP, Bio-Rad Laboratories) and with a template input of 10 ng (LHA/RHA and Drop-Off/TRAC) or 100 ng DNA (EIF2C1 and Drop-Off/TRAC) per reaction. The locked nucleic acid probe and the EIF2C1 primers and probe were

synthesized by Integrated DNA Technologies, and all other primers and hydrolysis probes were synthesized by Sigma-Aldrich. Primers were used at a final concentration of 900 nM and probes at 250 nM. Genomic DNA derived from leukocytes of healthy subjects was used as negative control, Sanger-sequenced plasmid DNA as positive control, and purified, nuclease-free water as no-template control in all ddPCR runs. The thermal cycling protocol was as follows: 10 min at 95°C, 40 cycles of 30 s at 94°C, 1 min at 60°C for annealing/extension, and one final step of 10 min at 98°C. For the LHA/RHA PCR, resulting in an amplicon of 2,337 bp, annealing/extension time was increased to 3 min. In-PCR digestion was performed with HindIII (LHA/RHA), HaeIII (EIF2C1), or MseI (Drop-Off/TRAC) in all cases. The plates were read on a QX200 droplet reader (Bio-Rad Laboratories) to determine droplet fluorescence intensity.

3.5.2 ddPCR data analysis

Droplets were manually assigned to double-negative, single-positive, or double-positive droplet clusters after visual inspection in QuantaSoft v1.7.4 (Bio-Rad Laboratories). Raw droplet fluorescence intensity values including cluster assignments were exported from QuantaSoft. Custom scripts were used to import the intensity values into R (version 3.4.4; http://www.r-project.org), to generate plots, and to quantify sample concentrations. Target concentrations were calculated for each well from the number of positive droplets Np and negative droplets Nn and the average droplet volume V = 0.85 nl based on Poisson distribution statistics using the formula c = (ln(Np + Nn) – ln(Nn))/V, where ln is the natural logarithm. Following Mock, Hauber, and Fehse (2016), rain droplets were considered negative because they represent mutated alleles. Gene-editing frequencies were calculated as the ratio of edited over edited plus wild-type allele concentrations.

3.6 *In vitro* functional assays

3.6.1 Luciferase-based co-culture cytotoxicity assay

12 days after gene electroporation and/or transduction, modified T cells were co-cultured with ML-2 target cells expressing the antigen recognized by TCR2.5D6 when presented on HLA-B7. ML-2 cells – an AML cell line – were transduced with a gene encoding Firefly luciferase (*fluc*) and HLA-B7 or HLA-B15 as a negative control. 10^4 target cells were co-cultured with T cells as the indicated effector-target cell ratio in 200 µl cytokine-free T cell medium at 37°C for

24h. As the knock-in efficiency and retroviral transduction efficiency differed, cells were diluted with non-modified T cells so that all test conditions contained the same fraction of TCRmu$^+$ T cells (murinized αβ-TCR positive T cells) and the same absolute number of T cells. For the effector-target cell ratio calculation, the number of TCRmu$^+$ T cells was used as the effector count. After co-culture, cells were pelleted and the supernatant was harvested and frozen at -20°C for IFN-γ secretion analysis. The cell pellet was gently resuspended in 100 µl prewarmed Luciferin solution, consisting of DPBS (Thermo Fisher Scientific), 10% FCS, and 150 µg/ml D-luciferin (Gold Biotechnology), and luminescence was determined on a VICTOR Multilabel Plate Reader (PerkinElmer) immediately afterwards. This assay relies on the assumption that only living, *fluc*-expressing target cells produce luminescence and the luminescence intensity is thus a measure of living tumor cells after co-incubation. Tumor cell lysis was determined as:

$$tumor\ lysis = (1 - (luminescence_{sample} \,/\, luminescence_{untreated\ tumor\ cells}) * 100)$$

Negative lysis indicates cell growth compared with the untreated tumor cell controls.

3.6.2 Enzyme-linked Immunosorbent Assay (ELISA)

The IFN-γ concentration secreted by the T cells into the supernatant during co-culture was determined using the Human IFN-γ ELISA Kit (BD) following the manufacturer's recommendations. Briefly, ELISA plastic plates were coated with 50 µl of anti-IFN-γ (1:250) diluted in coating buffer (see media and buffers section) over night at 4°C with a sealing foil to prevent evaporation. The next day, the plates were washed 3 times with washing buffer (see media and buffers section). Subsequently, the plates were blocked for 1h with 200 µl 1% milk powder in DPBS at room temperature under a sealing foil and washed 5 times. Next, a serial-dilution IFN-γ standard of 50 µl each in duplicates is added in two rows as a reference (1000 pg/mL, 500 pg/mL, 250 pg/mL, 125 pg/mL, 62,5 pg/mL, 31,25 pg/mL und 0 pg/mL). Samples were diluted 1:10 in DPBS and added in triplicates, each 50 µl. Samples and IFN-γ standard were incubated for 1h at room temperature under a sealing foil. For antigen detection, the plates were first washed 5 times and 50 µl of detection solution, consisting of 1% milk powder in DPBS, detection antibody (1:250), and enzyme conjugate (1:250), were added and incubated for 1h at room temperature. The plates were washed 7 times. Substrate solution was made by mixing equal volumes of BD OptEIATM TMB Substrate Reagent (BD

Biosciences) and 100 µl of subtrate solution were added. Plates were incubated at room temperature in the dark for 20 minutes and the reaction was stopped by adding 50 µl of sulfuric acid once the wells with the IFN-γ standard started turning blue. For quantification, the absorption at 450nm (λ correction 570 nm) was measured with a Sunrise Fotometer (Tecan) within 30min after stopping the enzymatic reaction. To determine the IFN-γ concentration of the samples, a linear regression was performed on the log-transformed IFN-γ standard concentrations and their respective log-transformed optical density.

3.7 Tumor xenograft mouse model

The *in vivo* experiment was based on a previously established tumor xenograft model (Mall et al., 2016; Mayer et al., 2018; Yusufi et al., 2017). Mice used for this experiment were maintained according to the institutional guidelines and approval of the local authorities. 8-12 weeks old NOD.CG-Prkdc^{scid} IL2rgtm^{1Wjl}/SzJ (NSG; The Jackson Laboratory) mice received a subcutaneous injection of 10^7 ML-2-B7 *fluc* cells – the same cell line that was used for *in vitro* functionality assays – in the right flank. On day 8 macroscopic tumor formation was visible and the animals were randomly assigned to the treatment or control groups. On days 8, 9, and 10, a total of 2 x 10^7 TCRmu$^+$ T cells were injected via tail-vein injection in 3 doses of 6.67 x 10^6 TCRmu$^+$ T cells 200 µl each. To account for different transduction and knock-in efficiencies, cell numbers and concentration of TCRmu$^+$ T cells were harmonized between treatment conditions with mock-transduced T cells. Tumor size was measured daily with a caliper and tumor area was calculated based on the following formula:

$$tumor\ area = tumor\ length * tumor\ width$$

Mice were euthanized on day 15 after tumor cell injection via isoflurane sedation and neck dislocation and tissues were harvested for histological analysis.

3.8 Histology and immunohistochemistry

Histology and immunohistochemistry were performed and described by Anja Ammer (previously Stelzl) and the stained slides were evaluated by PD Dr. Katja Steiger, an experienced certified pathologist. The following description of these methods has previously been published (Albers et al., 2019).

Directly after euthanasia of the mice, tissues were fixed in 4% neutral-buffered formalin solution for at least 48 h, dehydrated under standard conditions (ASP300S; Leica Biosystems) and embedded in paraffin. Serial 2-µm-thin sections prepared with a rotary microtome (HM355S; Thermo Fisher Scientific) were collected and subjected to histological and immunohistochemical analysis. Hematoxylin-eosin staining was performed on deparaffinized sections.

Immunohistochemistry was performed with a BenchMark XT automated stainer (Ventana) with an antibody against CD3 (103R-95, MRQ-39), using the ultraVIEW DAB Detection kit (all reagents were from Ventana). Briefly, the tissue sections were deparaffinized with EZ Prep at 75°C and 76°C, heat-pretreated in Cell Conditioning 1 (CC1) solution for antigen retrieval at 76°C–100°C and then incubated with the primary antibody diluted in antibody diluent 1:500 for 32 min at 37°C after inactivation of the endogenous peroxidase using a UV inhibitor for 4 min at 37°C. The slides were incubated with an HRP Universal Multimer for 8 min. Antibody binding was detected using DAB as chromogen and counterstained with hematoxylin for 10 min with subsequent bluing in bluing reagent for 10 min. The slides were then manually dehydrated by alcohol washes of increasing concentrations (70%, 96%, and 100%) and xylene and cover-slipped using Pertex mounting medium (00801; Histolab). The stained slides were evaluated by an experienced certified pathologist (PD Dr. K. Steiger) using a BX53 stereomicroscope (Olympus) and scanned using a slide scanner (AT-2; Leica Biosystems). Representative images were collected using Aperio Imagescope software (version 12.3; Leica Biosystems).

3.9 Statistics

Statistical analyses were performed using GraphPad Prism 7, as described in the figure legends. Error bars in all figures represent mean ± SD. Asterisks indicate statistical significance: * p = 0.01–0.05, ** p = 0.001–0.01, *** p = 0.0001–0.001, and **** p < 0.0001.

4. Results

4.1 Targeted integration of a tumor-reactive TCR in the *TRAC* locus replaces the endogenous TCR

First, we set out to test whether the endogenous TCR can be effectively replaced by a tumor-reactive exogenous TCR using a knock-in approach with CRISPR-Cas9 and AAV6. To induce the necessary DSB, we electroporated activated, primary human $CD8^+$ T cells with Cas9 RNPs. As the variable (V) and joining (J) region of the rearranged TCR α-chain gene differ from cell to cell, we targeted the constant region of the TCR α-chain (*TRAC* locus). We designed a gRNA binding within the first exon of the locus, upstream of the transmembrane domain, which associates with the β-chain to enable translocation of the TCR αβ-duplex to the cell membrane. This way, the peptide remnant of the endogenous TCR, which is still expressed after successful transgene integration, should not bind the endogenous β-chain and thus not be translocated to the surface **(Figure 4)** (Eyquem et al., 2017). We decided to use electroporated RNPs to induce the desired DSB as they have previously been shown to work well in primary human T cells, are ready to act without any further intracellular processing steps (e.g., translation, RNP assembly), and are rapidly degraded which leads to a shorter time of action and thus fewer off-target DSBs (Bernard et al., 2022; Schumann et al., 2015; Seki & Rutz, 2018).

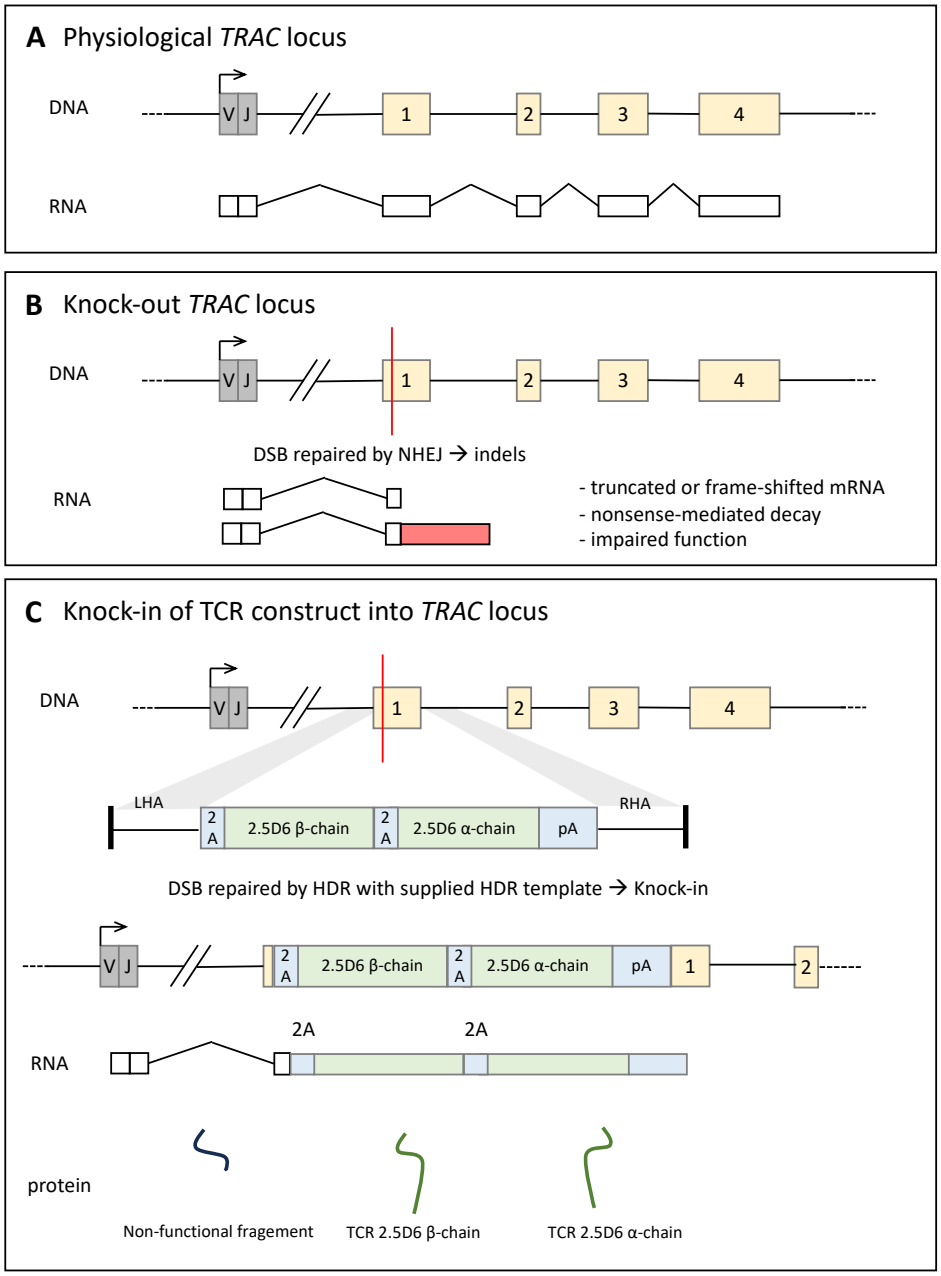

Figure 4: Schematic representation of the results of editing the endogenous *TRAC* locus
(A) Under physiological conditions, the expression of the rearranged TCR α-chain is driven from the promoter upstream of the Variable segment (V-segment). Notably, the used variable segment (V) and, therefore, the exact promoter used differs between T cells. The rearranged variable and Joining segment (J-segment) are then spliced together with the four exons of the constant region (*TRAC* locus). **(B)** When a DSB is induced in the first exon, in most cases the T cell will use nonhomologous end-joining (NHEJ) to repair it. This commonly induces indels. The indels can lead to a frameshift or introduces a premature stop codon. As a consequence, the resulting mRNA can be modified, truncated, or subjected to nonsense-mediated decay (NMD), which all impair the physiological expression and function of the endogenous TCR α-chain. **(C)** In the desired TCR knock-in scenario, a DSB is introduced and repaired by HDR in the presence of the HDR template encoding the transgenic TCR2.5D6. After corrected integration, the transgene is placed within the first exon of the *TRAC* locus. When transcription from the V promoter is initiated, an mRNA is formed and spliced that encodes for three proteins: (1) the truncated, non-functional remnant of the endogenous TCR α-chain, (2) the TCR2.5D6 TCR β-chain, and the TCR2.5D6 TCR α -chain. Schematic is based on graphics in (Albers et al., 2019; Eyquem et al., 2017; Schober, Muller, & Busch, 2020)

We observed an average knock-out efficiency of 51% in flow cytometry **(Figure 5A)**, defined as the difference between the mean fraction of TCRhuman$^-$ T cells after electroporating primary human T cells with RNPs containing the *TRAC* gRNA-compared to a non-targeting gRNA control. To further confirm and quantify the knock-out on the genomic level, we designed a ddPCR drop-off assay in which two fluorescently labeled probes bind to the *TRAC* locus: one spanning the CRISPR-cut site (Drop-off probe) and one binding outside of it (*TRAC* probe) **(Figure 5B)** (Mock, Hauber, & Fehse, 2016). When analyzing the genomic DNA from a genetically edited population of T cells, the editing efficiency can be calculated by comparing the fraction of molecules on which both probes bind (unedited) with that of molecules on which only the *TRAC*-probe binds, while the drop-off probe does not due to sequence-changes induced by indels after editing. On a genomic level, the mean editing efficiency was 40% **(Figure 5C, D)**, approximately in line with the flow cytometry results.

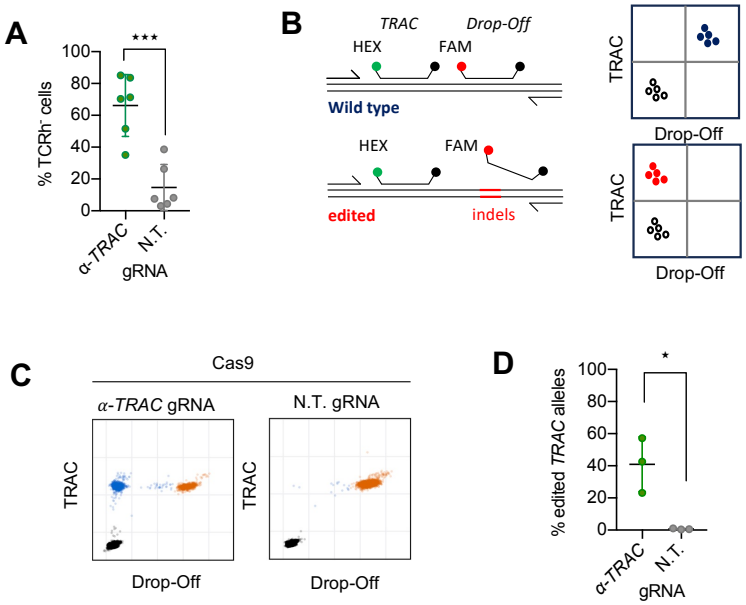

Figure 5: CRISR-Cas9 mediated TCR α-chain knock-out
Primary human CD8$^+$ T cells were electroporated with RNPs targeting the first exon of the *TRAC* locus (α-*TRAC*) or a non-targeting control (N.T.) and analyzed after 7 days of *ex vivo* culture. **(A)** Flow cytometric knock-out quantification based on the fraction of cells not expressing the human αβ-TCR (TCRh$^-$). Data represent three donors in two independent experiments, n = 6. **(B)** Schematic representation of the *TRAC* drop-off assay to determine editing frequency. **(C, D)** ddPCR analysis of editing frequency in genomic DNA 7 days after electroporation. 10ng genomic DNA input. **(C)** Representative visualization. x and y axes show fluorescence intensity (arbitrary units). **(D)** Quantification of the knock-out efficiency, n=3. Asterisks indicate statistical significance as determined by two-tailed unpaired t-test. Adapted from (Albers et al., 2019). Schematic based on (Mock, Hauber, & Fehse, 2016).

Next, in order to knock-in the tumor-reactive TCR2.5D6 into the desired DSB in the *TRAC* locus, we added AAV6s containing the HDR template to the T cells directly after the electroporation with RNPs. The HDR template consists of the bicistronic TCR2.5D6 construct which is flanked on both sides by approximately 900 bp long homology arms **(Figure 4)**. The α-chain and the β-chain of the construct are separated by a self-cleaving P2A element for equimolar expression from the same mRNA. The constant regions of both chains are murinized, an additional cysteine-bridge between them is added for enhanced stability, and both chains are codon-optimized for enhanced expression (Klar et al., 2014). We made use of a promoter-trap mechanism by placing another P2A element upstream of the TCR construct, in-frame with the open reading frame of the endogenous TCR α-chain: After correct integration, the expressed mRNA is multicistronic and is translated to a truncated peptide containing the Variable- (V-) and Joining segment (J-segment), the TCR2.5D6 α-chain and the TCR2.5D6 β-chain – all under the same transcriptional regulation of the endogenous promoter located upstream of the respective V-segment (Eyquem et al., 2017).

We chose AAV of the serotype 6 for HDR template delivery, as previous studies had demonstrated its tropism for primary human T cells and as AAVs are established tools to deliver relatively large constructs to the nucleus and thus the necessary place to enable HDR-mediated gene insertion at the intended DSB (Eyquem et al., 2017; Hale et al., 2017; MacLeod et al., 2017). Furthermore, AAV6 tends to deliver its cargo episomally to the nucleus, usually without relevant rates of autonomous genomic integration in human cells (D. Wang, Tai, & Gao, 2019). This is desirable in our setting to prevent transgene integration at unintended locations. As HDR is mainly restricted to the S phase and the G2 phase of the cell cycle (Scully et al., 2019; Takata et al., 1998), we used activated and thus proliferating primary human T cells for our experiments. Furthermore, the experiments were performed with $CD8^+$ T cells because the TCR2.5D6 recognizes its epitope – the tumor-associated peptide derived from myeloperoxidase – in an HLA-B7 (an HLA class 1 isotype) dependent manner (Klar et al., 2014).

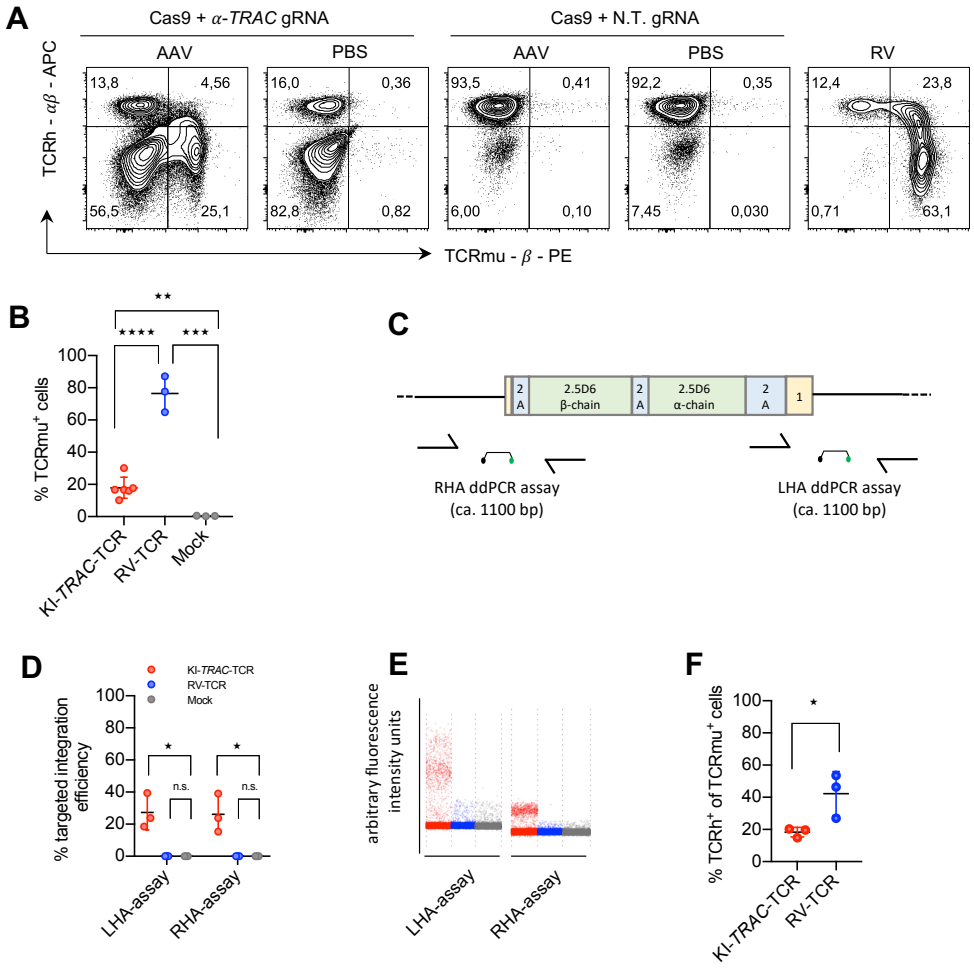

Figure 6: Knock-in of the murinized TCR2.5D6 into the *TRAC* locus
Primary human CD8 T cells were electroporated with α-*TRAC* or N.T. RNPs and transduced with AAV (MOI = 10^6) or PBS, or γ-retrovirally transduced. Cells and genomic DNA was analyzed 7 days after electroporation or transduction. **(A)** Representative flow cytometry plots. Axes use biexponential scaling. Graphs are 10% contour plots with outliers displayed. **(B)** Flow cytometry quantification of TCR knock-in T cells (KI-*TRAC*-TCR, data represent three donors in two independent experiments, n = 6), γ-retrovirally (retrovirally transferred TCR (RV-TCR), n = 3 donors), or mock-transduced cells (n = 3 donors). **(C)** Schematic of the ddPCR assays to quantify correct genomic integration with assays spanning the left (LHA-assay) or right homology arm (RHA-assay). **(D)** ddPCR quantification of the targeted integration efficiency (n = 3). **(E)** Representative visualization of the two ddPCR assay results. **(F)** Flow cytometry analysis as in **(A, B)**, n = 3 donors. Asterisks indicate statistical significance as determined by two- tailed unpaired t-test. Based on (Albers et al., 2019).

We observed TCRmu expression in T cells electroporated with *TRAC*-targeting RNPs and infected with donor-template bearing AAV6 (knock-in conditions) but not in the control conditions without the intended DSB or without AAV6 infection **(Figure 6A)**. This indicates that in the knock-in condition, the transgene is integrated into the *TRAC* locus as intended and is expressed from the endogenous TCR α-chain promoter. The mean knock-in efficiency (fraction of TCRmu$^+$ cells in flow cytometry) was 18% **(Figure 6A, B)**.

To confirm the targeted integration of the transgene at the intended genomic locus we designed two ddPCR assays to analyze the genomic DNA of edited T cells. In each assay an amplicon is generated spanning one homology arm with one primer binding within the TCR2.5D6 construct and one primer binding outside of the 900 bp of the homology arm. Thus a PCR amplicon can only be produced if the transgene has integrated at the correct position, not from the episomally located HDR template **(Figure 6C)**. Targeted genomic integration was exclusively observed in the KI conditions, with a mean integration efficiency of 27%, and not in the retrovirally transduced conditions **(Figure 6D, E)**. Since the TCR α-chain is functionally monoallelically expressed in most T cells (due to allelic exclusion), transgenes integrated into the inactive *TRAC* locus would not lead to TCR2.5D6 surface expression (Brady, Steinel, & Bassing, 2010; Corthay, Nandakumar, & Holmdahl, 2001). This explains the higher knock-in rates observed in ddPCR compared to flow cytometry.

To test, whether the knock-in replaces the endogenous TCR with the introduced one, instead of merely adding it, we compared the fraction of $TCRmu^+$ T cells that still express the endogenous TCRhuman in knock-in conditions and retrovirally transduced conditions. Notably, this "double-positive fraction" was significantly reduced in the knock-in condition to a mean of 18% compared to a mean of 41% in the retrovirally transduced conditions **(Figure 6A, F)**.

In summary, these findings demonstrate the targeted integration of the tumor-reactive TCR2.5D6 into the *TRAC* locus at a reasonable knock-in efficiency, leading to a replacement of the endogenous TCR by the introduced one and transcription from the endogenous promoter.

4.2 TCR knock-in redirects T cell specificity against tumor cells *in vitro*

After showing that the knock-in had equipped the T cells with the new TCR and that this new TCR is expressed on the cell surface, we tested whether the T cells could now also recognize the corresponding antigen *in vitro* or whether they had lost functionality as a result of the intervention. For this, we co-incubated knock-in T cells with ML-2 AML cells that express myeloperoxidase – the protein of which a peptide fragment is recognized by the introduced

TCR2.5D6 when expressed on HLA-B7 – at different T cell-target cell ratios for 24h. Modified T cells selectively lysed tumor cells transduced with HLA-B7 but not those transduced with HLA-B15 as a control, while non-modified T cells did not show any cytotoxicity, demonstrating the TCR- and HLA-dependent cytotoxicity of the modified T cells **(Figure 7A)**. When compared to retrovirally transduced T cells or retrovirally transduced TCRendo^{-} knock-out T cells, no notable differences in their *in vitro* cytotoxicity **(Figure 7B)** or INF-γ secretion **(Figure 7C)** were seen.

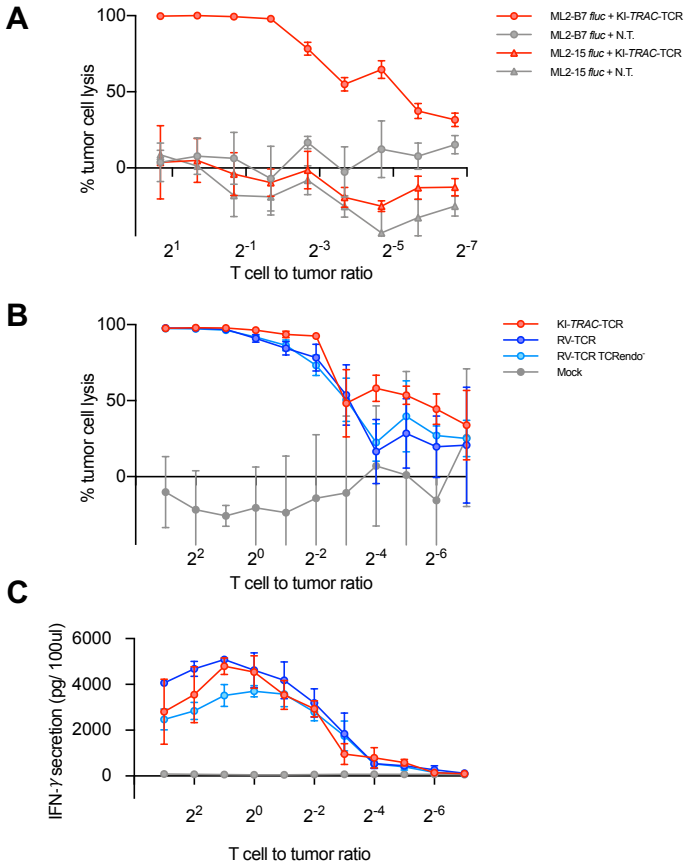

Figure 7: TCR2.5D6 knock-in redirects T cell specificity *in vitro*
(A) Tumor cell lysis of *fluc* expressing ML-2 cells transduced with HLA-B7 or as a negative control HLA-15 after 24h co-culture at the indicated ratios with TCR2.5D6 TCR knock-in T cells or T cells electroporated with non-targeting RNPs and AAV6 as a negative control. n = 3, technical replicates of 1 donor. **(B)** Luciferase cytotoxicity assay comparing KI-*TRAC*-TCR cells, RV-TCR, RV-TCR TCRendo^{-}, and mock transduced T cells after 24 h of co-incubation with ML-2-B7 *fluc* at indicated T cell to tumor ratios. Different amounts of mock transduced T cells were added to each condition so that equal fractions of TCRmu^{+} cells, and equal numbers of TCRmu^{+} cells and total T cells were used for co-incubation in each test condition. n = 3, technical replicates of 2 donors. **(C)** IFN-γ ELISA of the supernatant of **(B)**. Asterisks indicate statistical significance as determined by two-tailed unpaired t-test. Based on (Albers et al., 2019).

4.3 TCR knock-in T cells effectively reject xenograft tumors in an *in vivo* mouse model

Next, we tested whether the TCR knock-in T cells are capable of defeating a xenograft tumor in an *in vivo* setting. For this, we used a previously established mouse xenograft model (Mall et al., 2016; Mayer et al., 2018; Yusufi et al., 2017): ML-2-B7 *fluc* cells – the same that were used for the *in vitro* studies – were subcutaneously injected into the flank of NSG mice. When macroscopic tumors were established after 8 days, TCR knock-in T cells, retrovirally transduced T cells, retrovirally transduced TCRendo$^-$ knock-out T cells, mock transduced T cells or PBS were intravenously injected in three portions over three days. Since the different T cell modification methods have different efficiencies, retrovirally transduced T cell conditions were diluted with mock-transduced T cells to make sure that in all test conditions (TCR knock-in, RV, RV TCRendo$^-$) the same number of T cells and the same number of TCRmu$^+$ T cells (and thus the same fraction of TCRmu$^+$ T cells) were injected.

Within 7 days the tumor burden was equally reduced in all three test conditions **(Figure 8A)** and in most mice, no tumors were macroscopically detectable after this time **(Figure 8B)**. In mice injected with mock-transduced T cells or PBS, the tumors continued to grow.

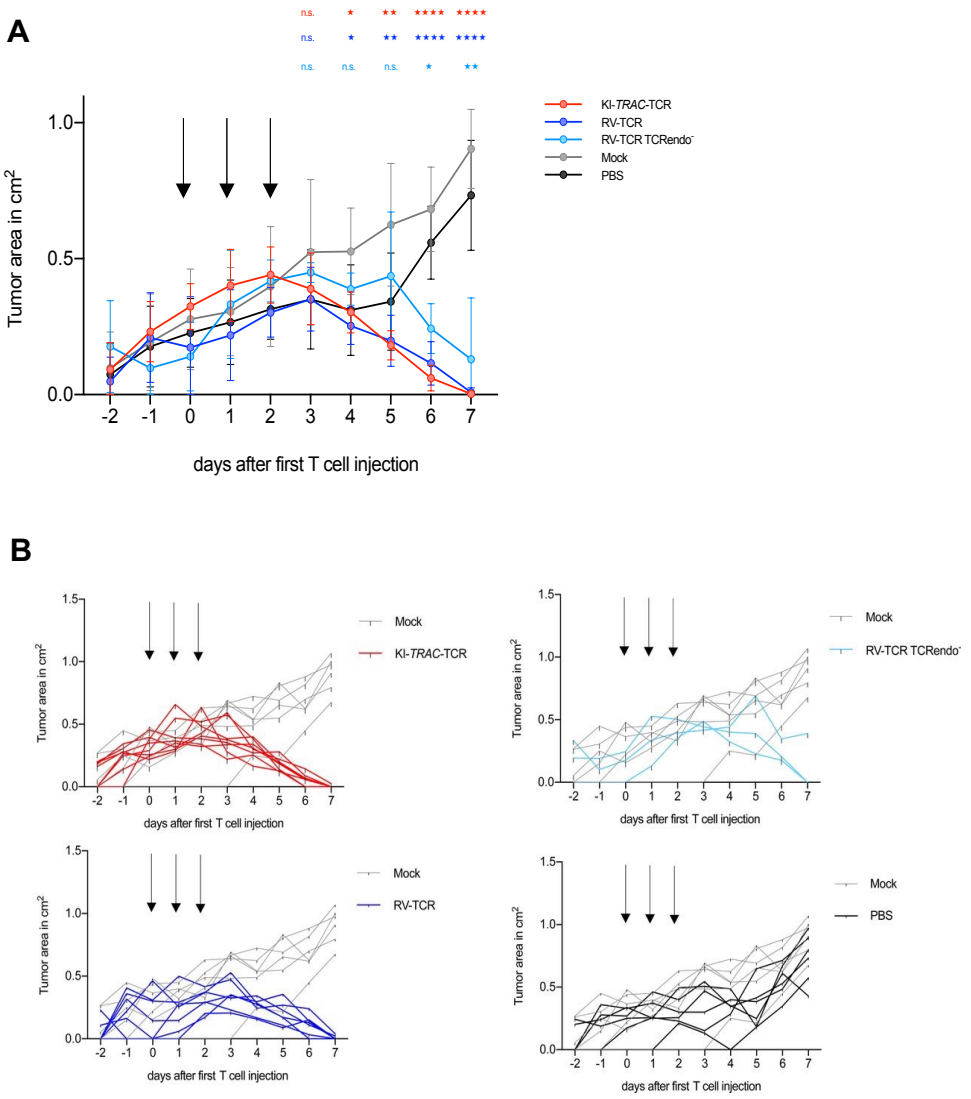

Figure 8: TCR2.5D6 knock-in T cells potently reject antigen-bearing tumors *in vivo* in a ML-2 xenograft mouse model

(A) NOD.CG-Prkdc^{scid} IL2rg^{tm1Wjl}/SzJ (NSG) mice bearing subcutaneous xenograft ML-2-B7 *fluc* tumors were treated with the intravenous adoptive transfer of 2 × 10^7 TCRmu$^+$ KI-*TRAC*-TCR T cells (n = 8), RV-TCR T cells (n = 7), RV-TCR TCRendo$^-$ T cells (n = 3), mock transduced T cells (n = 6) derived from one donor, or PBS (n = 6). Arrows indicate the injection of 6.67 × 10^6 TCRmu$^+$ T cells in 200 µl PBS. Asterisks indicate statistically significant differences in tumor area of the test conditions compared to mock transduced T cells as determined by multiple t-tests corrected for multiple comparisons using the Holm–Sidak method. **(B)** Tumor area of the individual mice. one line = one mouse. Based on (Albers et al., 2019).

Upon pathological evaluation, a strong infiltration of CD3$^+$ cells but almost no residual tumor cells were observed at the site of subcutaneous tumor injection in the conditions treated with i.v. TCR knock-in, retrovirally transduced or retrovirally transduced TCRendo$^-$ knock-out T cells, while almost no infiltration was observed in the tumors exposed to the control conditions

(Figure 9). Thus, within this xenograft model, TCR knock-in T cells migrated to the tumor and controlled it equally well as retrovirally transduced T cells.

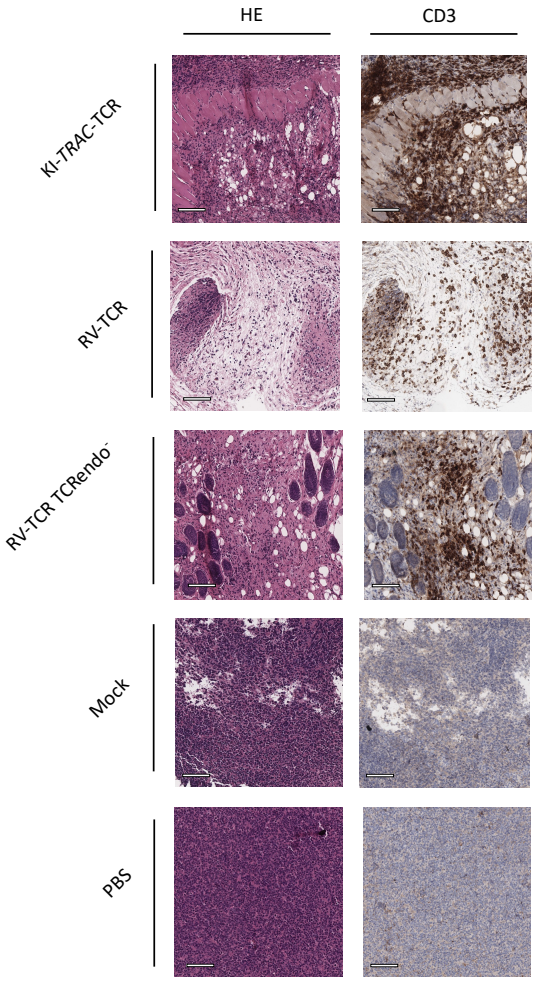

Figure 9: T cells infiltrate the xenograft injection site after TCR2.5D6 knock-in in T cells
Representative Hematoxylin and eosin stain (HE) and CD3 stains of the ML-2-xenograft injection site derived from the mice treated with TCRmu^{+} KI-*TRAC*-TCR T cells, RV-TCR T cells, RV-TCR TCRendo^{-} T cells, mock transduced T cells, or PBS. Microscopic evaluation and choice of representative images were performed by an experienced pathologist (K. Steiger, Institute of Pathology, TUM). Scale bars, 100 µm. Based on (Albers et al., 2019)

5. Discussion

We demonstrated that a tumor-reactive TCR can genetically and functionally replace the TCR of primary human T cells by integrating the transgenic TCR into the endogenous *TRAC* locus. Using CRISPR-Cas9 RNPs to induce the intended DSB and AAV6 to deliver the repair template, we achieved a reasonable knock-in efficiency of ~18%. The engineered T cells recognized and killed tumor cells *in vitro* and *in vivo* in an AML xenograft tumor model. In this preclinical test setting, TCR knock-in T cells demonstrated equal cytotoxicity, IFN-γ secretion, and *in vivo* functionality as retrovirally transduced T cells.

5.1 Is targeted TCR replacement superior to conventional viral gene transfer?

We hypothesized that the targeted integration of a TCR in the *TRAC* locus has advantages compared to the semi-random integration pattern of retroviruses in three key points: (1) reduced genotoxicity due to a controlled integration in a safe locus, (2) a replacement of the endogenous TCR instead of a mere addition, and (3) an improved function of the knock-in T cells due to the usage of the endogenous transcriptional regulation.

5.1.1 Genotoxicity

The HDR template encoding TCR2.5D6 does not carry an exogenous promoter but relies on a promoter trap mechanism to drive the transgene expression from the endogenous *TRAC* promoter. The expression observed in flow cytometry is, therefore, driven either from the *TRAC* promoter or a different endogenous promoter at a site of wrongful integration of the targeting construct. The ddPCR assay further demonstrated that some transgenes integrated into the *TRAC* locus as intended. However, we did not specifically identify or quantify integration at unintended sites of the genome. This can be tested with targeted locus amplification (TLA), a method to map insertion sites and structural variation throughout the genome (de Vree et al., 2014). Others analyzed TCR knock-in or CAR knock-in T cells with TLA and observed the integration into the intended locus to be highly specific without off-target hot spots, while integration sites of retrovirally transduced transgenes were dispersed throughout the genome (Eyquem et al., 2017; Müller et al., 2021; Roth et al., 2018; Schober et al., 2019). In knock-in conditions, off-target integration mainly occurred in a homology-independent way at off-target DSBs. Off-target integrations in sites without DSBs were

observed much less (Roth et al., 2018) or not at all within the methodology‘s detection limit (Schober et al., 2019). Notably, the off-target integration rate depended on the type of HDR template supplied. Roth et al. (2018) noted that the already low off-target integration rate of 0.1% for dsDNA templates could be reduced to 0.01% using a Singe-strand DNA (ssDNA) template. Therefore, the knock-in of transgenes in primary human T cells can be regarded as highly specific. Furthermore, despite some off-target integration events, the method is still significantly more specific than semi-randomly integrating retroviruses (Müller et al., 2021).

The clinical relevance of this finding is debatable. In a few early clinical trials of gammaretroviral transduction of hematopoietic stem cells (HSCs) for the correction of X-linked severe combined immunodeficiency (SCID-X1), patients developed T-cell lineage hematologic malignancies due to insertional mutagenesis, which fueled significant reservations about the technology (Cavazza, Moiani, & Mavilio, 2013; Hacein-Bey-Abina et al., 2003; Poletti & Mavilio, 2018). However, despite decade-long experience with genetically engineered mature T cells (Melenhorst et al., 2022; Schober, Muller, & Busch, 2020; Scholler et al., 2012), only two cases of transformed T cells were observed (Micklethwaite et al., 2021; Schambach, Morgan, & Fehse, 2021). In both cases, T cells were engineered via *piggyBac* transposons after matched-related allo-HSCT, and patients developed donor-derived T cell lymphomas. While the exact reason for transformation in these cases is not fully understood, it might be related to the abnormally high VCN found in the engineered cells of affected patients or the semi-random integration pattern of *piggyBac* transposons with a preference for transcriptional start sites, promoter-, and enhancer-sequences. All U.S. Food and Drug Administration (FDA) approved CAR-T cell therapies are based on γ-retroviral (axicabtagene ciloleucel, brexucabtaene autoleucel) or lentiviral vectors (tisagenlecleucel, lisocabtagene maraleucel, idecabtagene vicleucel, ciltacabtagene autoleucel) (Berdeja et al., 2021; Poletti & Mavilio, 2018). In general, mature T cells seem less prone to oncogenic transformation than HSCs (Ferrari, Thrasher, & Aiuti, 2021; Newrzela et al., 2008).

On the other hand, the induction of DSB at intended target- or unintended off-target sites comes with a set of other unwanted downsides. CRISPR-Cas9 does not exclusively bind and cut the intended site but also off-target sites with a high sequence similarity (Kaeuferle et al., 2022; Wienert & Cromer, 2022; X. H. Zhang, Tee, Wang, Huang, & Yang, 2015). These off-target

DSBs can functionally impair the affected sequence and increase the risk of translocations due to the higher number of simultaneously occurring DSBs. Off-target DSBs strongly depend on the specificity of the gRNA chosen and the genetic background of the donor T cells. They should, therefore, ideally be selected in a personalized way (Lessard et al., 2017). Several approaches are being used to reduce off-target cleavage, such as optimal gRNA design, shortening the time window of Cas9 activity by using RNPs, and engineered high-fidelity Cas9 variants (Bernard et al., 2022). This way, off-target cleavage can be reduced but not eliminated.

Besides off-target cleavage, structural genomic abnormalities are regularly observed in gene-edited cells. These include translocations (Stadtmauer et al., 2020), large deletions (Adikusuma et al., 2018; Kosicki, Tomberg, & Bradley, 2018), loss of heterozygosity (Alanis-Lobato et al., 2021), chromothripsis (Leibowitz et al., 2021) and chromosome loss (Nahmad et al., 2022; Tsuchida et al., 2023). The risk of chromosomal aberrations is further aggravated if several DSBs are simultaneously induced, as has been done in several *in-human* studies (Bonini et al., 2023; Stadtmauer et al., 2020). The factors governing the occurrence, functional consequences, and risks of many of these effects are still unclear. For translocation and chromosome loss, however, strategies to minimize their occurrence and impact have been developed, such as serial instead of simultaneous editing, the use of base-editors that do not induce DSBs, or optimized T-cell editing protocols with activation after instead of before RNP electroporation (Tsuchida et al., 2023).

Despite these unknowns, numerous *in-human* studies using CRISPR-Cas9 edited T cells have been completed or are currently ongoing (Bonini et al., 2023). The clinical experience gained in these studies will help to better assess the risk profile of genome-edited T cells and compare it to that of established gamma-retroviral and lentiviral transduction.

5.1.2 TCR replacement instead of addition

Most T cells bear a single αβ-TCR because the TCR α- and β-chains are each selectively expressed from only one of the tow alleles, a process called allelic exclusion. This is true for the majority of cases, but approximately 5% of T cells naturally express two different TCRs

(Corthay, Nandakumar, & Holmdahl, 2001). When retrovirally introducing a transgenic TCR into a T cell, two different α-chains and two-different β-chains are expressed (one each from the endogenous TCR and the introduced one). This comes with two disadvantages: They (1) compete for surface expression and (2) could potentially bind in unexpected combinations leading to mismatched heterodimeric receptors with new, potentially autoreactive, specificities (Bendle et al., 2010). As outlined in the introduction, several approaches have been developed to reduce this. We reasoned that by knocking the murinized TCR2.5D6 into the *TRAC* locus, we would achieve two goals at once by not only introducing the new TCR but also preventing the expression of the endogenous TCR α-chain. As the introduced TCR bears murinized constant regions, we reasoned that in an optimal scenario, the intact endogenous β-chain would not have a binding partner left. Thus, only the introduced TCR would be expressed at the cell surface.

Indeed, the fraction of $TCRmu^+$ T cells that also express the endogenous TCRhu (TCRhu-TCRmu-double-positive fraction) is significantly lower in the TCR knock-in T cells (~18%) than in the retrovirally transduced T cells (~41%) based on the manually chosen cut-off in flow cytometry **(Figure 6A, F)**. These TCRhu-TCRmu-double-positive T cells formed a distinct population in the retrovirally transduced condition. In contrast, not any clearly demarcated TCRhu-TCRmu-double-positive population was observed in the TCR knock-in conditions. Eyquem et al. (2017) observed that approximately 5% of CAR^+ T cells still expressed the endogenous TCR after knocking-in a CAR into the *TRAC* locus, which is in line with the 5% of naturally occurring TCR-double positive T cells (Corthay, Nandakumar, & Holmdahl, 2001). The fact that the TCRhu-TCRmu-double-positive rate after TCR2.5D6 knock-in was higher than 5% could be attributed to the formation of mismatched TCR_{human}-β:$TCR_{2.5D6}$-α TCRs, which might still be bound by the anti-human TCRα/β antibody (BW242/412). BW242/412 recognizes an epitope of the constant region of the human TCR β-chain and thus also chimeric, mismatched TCRs that contain a human TCR β-chain (Kierkels et al., 2021). The mismatched TCR_{human}-β:$TCR_{2.5D6}$-α TCRs could form because the murinization of the TCR constant regions does not entirely exclude binding to human chains (Sommermeyer & Uckert, 2010). In a set of detailed comparisons of T cells edited in one or both endogenous TCR chains in combination with retroviral transduction or TCR knock-in, Schober et al. (2019) demonstrated that counterintuitively, the disruption of one TCR chain could even enhance the formation of

mismatched TCRs. In contrast, only the disruption of both endogenous chains entirely prevented TCR mismatch formation.

In summary, after knocking a murinized TCR into the *TRAC* locus, we observed a replacement instead of a mere addition of the transgenic TCR in most T cells, but most likely at the cost of an increased formation of mispaired TCRs. So far, no autoimmune consequences due to TCR mismatches have been found in clinical studies, so this might not be a relevant drawback for clinical translation, albeit there is limited clinical experience with TCR-transgenic ACTs (Schober et al., 2019). Nevertheless, future studies should use strategies to knock out both endogenous TCR chains – especially if fully human TCRs are used.

5.1.3 Functional consequences of using the endogenous promoter

When conventional T-cell engineering strategies with semi-randomly integrating viral vectors are used, the transcription of the transgenic TCR or CAR is driven from an exogenous promoter. Eyquem et al. (2017) observed that CAR-T cells demonstrated superior *in vivo* tumor control and reduced exhaustion marker expression when a CAR was knocked into the *TRAC* locus and placed under endogenous transcriptional control compared to a retrovirally integrated CAR under the transcriptional control of an exogenous promoter. This difference was not observed in *in vitro* studies and only became apparent in a long-term xenograft tumor model (100 days observation length). Most notably, this advantage was only seen when the CAR was placed under endogenous transcriptional control, and not when the CAR was knocked into the *TRAC* locus but placed under the transcriptional control of an exogenous promoter. We hypothesized that – since the endogenous TCR α-chain promoter underlies evolutionary pressure for optimal T cell function – similar functional improvements could also be observed for T cells with a tumor-reactive TCR placed under the transcriptional control of the *TRAC* locus. However, in our setting, we did not see notable functional differences *in vitro* or *in vivo* between TCR knock-in T cells without and retrovirally transduced T cells with an exogenous MPSV-LTR promoter **(Figure 7, 8)**. This could be either attributed to a missing functional difference between the two or an inability of our set-up to detect such a difference. Eyquem et al. (2017) suggested that the dynamic transcriptional control of the *TRAC* locus reduces chronic signaling, thereby reducing T cell exhaustion and thus improving *in vivo* functionality. Since our *in vitro* and *in vivo* experiments only tested the early phase of the anti-tumor

response (24h and seven days, respectively), we would not have been able to detect differences in T cell exhaustion due to chronic stimulation.

The findings of other groups investigating the potential advantages of placing a transgenic TCR under the transcriptional control of the *TRAC* locus paint a mixed picture:
When knocking the tumor-reactive TCR NY-ESO-1 (New York esophageal squamous cell carcinoma 1) into the *TRAC* locus, similar *in vitro* cytokine secretion and cytotoxicity as with retrovirally transduced T cells were observed. However, when adoptively transferred to xenograft melanoma-bearing mice, a significantly improved tumor control was observed, starting at day 19, when compared to lentivirally transduced T cells (Roth et al., 2018). Schober et al. (2019) also did not see any differences *in vitro* in short-term target cell killing and cytokine secretion when comparing TCR knock-in T cells with retrovirally transduced ones. Still, in a set of comparisons with five different TCRs, they noted that TCR knock-in T cells showed a near-physiological regulation with transcriptional downregulation of the TCR upon antigen stimulation. A similar pattern had been observed for CARs when integrated in the *TRAC* locus (Eyquem et al., 2017). The functional consequence of this regulatory dynamic remains to be determined. Müller et al. (2021) further characterized the implications of placing the transgenic TCR under endogenous transcriptional control. They did so by comparing TCR knock-in T cells, in which in most cases only one transgene is actively being transcribed, to T cells retrovirally transduced at such a low MOI that following a Poisson distribution only one integrated transgene is to be expected. While similar surface expression levels were observed five days after editing, knock-in T cells expressed significantly higher levels of TCR after two weeks of *ex vivo* culture. At this time, TCR knock-in T cells showed higher *in vitro* cytotoxicity and cytokine production, which was probably a consequence of higher TCR surface expression. They further demonstrated that TCR knock-in led to a more homogeneous and predictable cell product, an essential quality parameter for cell therapy. Overall, however, evidence is missing that the transcriptional regulation of the endogenous TCR leads to superior *in vivo* functionality compared to exogenous promoters in conventionally engineered T cells for TCR transgenic ACT. A recent publication by Ruggiero et al. (2022) provides data that speaks against the superiority of the endogenous promoter. In an AML xenograft model, both knock-in TCR T cells using the endogenous *TRAC* promoter and the exogenous promoter EF1α controlled the tumor significantly better than lentivirally

transduced T cells (38 days). That said, the cells using the EF1α promoter had a more activated and less exhausted phenotype. It remains unclear if *in vivo* functionality differences would have been observed at later time points. Which T cell activity dynamic allows for the best clinical anti-tumor response will most likely also depend on the disease setting and the characteristics of the TCR. Long-term *in vivo* experiments with xenograft or syngeneic tumor models will be needed to further characterize these features.

5.2 Improvements of the TCR Knock-in Methodology

The T cell engineering field has made tremendous advancements in the last few years with further optimization and refinement of almost every step of the T cell production process. The advanced methodologies improve editing efficiencies and reduce manufacturing time – one of the key bottlenecks for clinical translation (Finck, Blanchard, Roselle, Golinelli, & June, 2022). In the following, I want to highlight some approaches that deviate from our methodology.

5.2.1 T cell subset and activation status

All our experiments were performed with activated $CD8^+$ primary human T cells without further selection of specific differentiation phenotypes. We decided to selectively work with this cell subset, as TCR2.5D6 recognizes its peptide in the context of the class I HLA-B7, and the *in vitro* and *in vivo* functionality of retro virally transduced TCR2.5D6 T cells were previously characterized in $CD8^+$ T central memory cells (T_{CM}) (Audehm et al., 2019; Klar et al., 2014). Our findings are thus potentially not generalizable to $CD4^+$ T cells – which were also shown to play an essential role in the anti-tumor immune response (Kruse et al., 2023) and are commonly included in the adoptive cell transfer (ACT) manufacturing process. Others have shown that the optimal conditions for gene editing of $CD8^+$ and $CD4^+$ T cells differ, both for knock-out and knock-in (Oh et al., 2022; Seki & Rutz, 2018), although with a consensus condition, both cell subsets can be edited at high rates (Roth et al., 2018; Schober et al., 2019). Several studies suggest the superiority of specific T cell differentiation phenotypes (e.g., naïve T cells, persistent central memory T cells) for ACT, even though the optimal phenotype seems to differ in different disease settings (Fraietta, Lacey, et al., 2018; Klebanoff, Gattinoni, & Restifo, 2012; Korell, Berger, & Maus, 2022). The fact that both $CD8^+$ and $CD4^+$ T cells can be

gene-edited well under the same conditions is favorable for clinical translation. All clinically approved ACT therapies use a mix of both subsets, with Lisocabtagene maraleucel being the only exemption using a fixed CD8/CD4 ratio (Abramson et al., 2020; Korell, Berger, & Maus, 2022). The selection of specific differentiation phenotype subsets is clinically less relevant, but early experience from clinical-grade manufactured non-virally edited T cells suggests that either the editing procedure or the targeted gene disruption shifts the cell product to more favorable T cell differentiation phenotypes (Foy et al., 2023; Stadtmauer et al., 2020; J. Zhang et al., 2022). More clinical experience with different T cell modifications is needed to gain clarity about this effect, the mechanisms behind it, and its clinical consequences.

For all our experiments, we activated the T cells prior to gene editing, reasoning that due to the induction of proliferation, more cells would be in S or G2 phase at the time of DSB induction. This should lead to more cells being capable of performing HDR at this moment, thus increasing the knock-in efficiency. However, it was recently demonstrated that this approach can lead to the loss of the edited chromosome, and activating T cells only after electroporation generates a potentially safer cell product for clinical translation (Tsuchida et al., 2023). It has been observed that editing the *TRAC* locus using a CRISPR-Cas9 editing protocol that includes T cell activation prior to electroporation leads to the loss of chromosome 14 (Nahmad et al., 2022). Tsuchida et al. (2023) confirmed that this effect is universally observed for edited loci throughout the genome (chromosome loss occurred in 3.25% of all edited T cells). Intriguingly, they noticed that chromosome loss was extremely low in the edited T cells administered in a first-in-human clinical study of CRISPR-Cas9 edited ACT, in which T cells were only activated after gene editing (Stadtmauer et al., 2020). They suggest that mechanistically, two factors could be at play: (1) activated T cells could be prone to chromosome loss after DSB induction due to transcription-dependent genome instability, or (2) activation-induced downregulation of p53 prevents it from inducing apoptosis in cells with aneuploidy and thus prevents selection against cells with chromosome loss. As knock-in efficiencies in non-activated T cells are significantly impaired, more research into the clinical risks of chromosome loss, and HDR-independent ways to knock in transgenes in T cells will be needed to weigh the risks and advantages of activating T cells before gene editing.

5.2.2 Improved Double-strand Break Induction

To induce DSBs at the intended locus, we used the most established Cas9 variant, *Streptococcus pyogenes* Cas9 (SpCas9), derived from *Streptococcus pyogenes*, delivered as electroporated RNPs (S. Kim, Kim, Cho, Kim, & Kim, 2014; Schumann et al., 2015). RNPs combine several advantages over the delivery of Cas9 as mRNA or DNA. In RNPs, the guideRNA is already bound to Cas9, which allows for immediate targeted endonuclease activity, prevents the otherwise fast degradation of guideRNAs, and leads to high editing rates (Hendel et al., 2015; S. Kim et al., 2014; Nguyen et al., 2020). Furthermore, due to its relatively short time of action before degradation (24-48h) compared to other Cas9 delivery methods, the off-target editing rate is reduced (S. Kim et al., 2014). Due to these factors, in combination with well-established T cell electroporation protocols that allow high editing efficiencies and preserve high cell survival, RNPs are the delivery method of choice for clinical settings today (Foy et al., 2023; Stadtmauer et al., 2020; J. Zhang et al., 2022). Since the discovery of SpCas9, several other Cas9 variants have been identified or engineered to recognize other PAMs or reduce off-target edits. Cas9 variants with other PAMs allow the editing of genomic regions that do not contain the SpCas9 PAM NGG (Bernard et al., 2022; Kleinstiver, Prew, Tsai, Nguyen, et al., 2015; Kleinstiver, Prew, Tsai, Topkar, et al., 2015; Miller et al., 2020; Walton, Christie, Whittaker, & Kleinstiver, 2020; Y. Wang et al., 2019). This will be more relevant for the preclinical study of specific potentially disease-causing variants than for the clinical editing of therapeutic T cells. To further increase Cas9 specificity and reduce off-target edits, several high-fidelity Cas9 variants have been engineered (Kleinstiver et al., 2016; Slaymaker, Gao, Zetsche, Scott, Yan, & Zhang, 2016; Vakulskas et al., 2018).

5.2.3 Improved Knock-in of Target Constructs

We used AAV6 to deliver the HDR template to the nucleus for targeted knock-in. AAV6 was chosen due to its ability to deliver relatively large HDR templates episomally to the nucleus of primary human T cells (Eyquem et al., 2017; Hale et al., 2017; MacLeod et al., 2017). Others developed completely non-viral approaches, in which the HDR templates are delivered as linearized or circular dsDNA or ssDNA samples and directly co-electroporated with the RNPs (Iyer et al., 2022; Nguyen et al., 2020; Oh et al., 2022; Roth et al., 2018; Schober et al., 2019). By adding Cas9 targeting sequences to the HDR template, Cas9 bearing a nuclear localization signal could be recruited to bind the HDR and shuttle it to the nucleus, further increasing

knock-in efficiencies (Nguyen et al., 2020; Shy et al., 2023). Additionally, small molecules to inhibit NHEJ make edited T cells preferentially use HDR to repair DSBs (Fu et al., 2021; Kath et al., 2022; Shy et al., 2023; Wienert et al., 2020). Non-viral genome targeting has been heavily optimized to enable high editing rates while keeping DNA toxicity low. Compared to AAV-based gene targeting, the cost and complexity of manufacturing non-virally engineered T cells are much lower, and the manufacturing process is much faster. This makes it easier to implement non-viral approaches under good manufacturing practice (GMP) conditions for clinical studies (Foy et al., 2023; J. Zhang et al., 2022). Furthermore, the fast and easy development of new receptor constructs, without the need to produce a different virus for each, allows the use of patient-specific receptors – which, as I will discuss in the outlook section, is an essential development to harness the power of targeting patient-specific tumor neoantigens (Foy et al., 2023).

The methodologies laid out here have been developed and improved within just a few years. Further improvements will follow. With the fast progress of clinical translation in mind, it will be essential to adhere as closely as possible to clinical-grade cell manufacturing protocols during preclinical development to being able to easily translate the findings to *in-patient* use (Tsuchida et al., 2023).

5.3 First clinical applications

The recent, tremendous advancements in completely non-viral gene editing technology have made targeted knock-outs or knock-ins easier to implement clinically under GMP conditions, cheaper, and faster than conventional T cell engineering methods. Only six years after the discovery of CRISPR-Cas9, the first patients were treated with CRISPR-edited T cells (Bernard et al., 2022; Stadtmauer et al., 2020). In a first-in-human phase 1 pilot-study three patients with advanced, refractory cancer (two with multiple myeloma, one with metastatic sarcoma) were treated with T cells that were lentivirally transduced with the tumor-reactive TCR NY-ESO-1 and CRISPR-Cas9 multiplex-edited to knock-out *TRAC*, T Cell Receptor Beta Constant 1 (*TRBC1*), T Cell Receptor Beta Constant 2 (*TRBC2*), and *PDCD1 (Stadtmauer et al., 2020)*. The gene editing was intended to reduce competition with the endogenous chains and mispairing, thereby increasing the expression of NY-ESO-1 and improving anti-tumor immunity. The authors aimed to test the feasibility and safety of multiplexed genome engineering in human

T cells. Manufacturing of edited T cells at clinical scale was feasible with varying knock-out efficiencies per target gene. The study suggested that using multiplexed edited T cells is safe; only mild side effects were observed, which can be attributed to the lymphodepletion therapy before T cell infusion. While patients showed pre-existing humoral and T cell reactivity to Cas9, infusion of the edited T cells did not lead to a humoral response, most likely due to almost no Cas9 protein left in the edited cells after *ex vivo* expansion. This indicates that rejection due to pre-existing immunity is no barrier to clinical translation. Off-target editing was very limited, and translocations were generally rare events (max. 6% of T cells showed a *TRBC1:TRBC2* translocation in one patient). Notably, the frequency of the tested translocations declined over time *ex vivo* and *in vivo*, indicating that they do not confer a growth advantage to T cells. While these findings suggest a generally good safety profile, experience with more patients and longer observation times will be necessary to assess this. Interestingly, multiplex-edited NY-ESO-1 T cells engrafted more, persisted longer, and expressed more genes associated with central memory than observed in other studies of NY-ESO-1 T cells without genome editing.

The targeted integration of antigen-receptors to a specific genomic locus has also reached the clinic. J. Zhang et al. (2022) used non-viral CRISPR-Cas9 mediated HDR to integrate an anti-CD19 CAR driven by an EF1α promoter into the *PDCD1* locus to treat eight patients with relapsed/refractory B cell non-Hodgkin lymphoma (r/r B-NHL). Clinical T-cell editing also showed a favorable safety profile in this setting. Mild and transient hematological toxicity events attributed to lymphodepletion and mild cytokine release syndrome in some patients were observed. Off-target editing was observed at low frequency in the *PHACTR1* (phosphatase and actin regulator 1) locus, a gene not expressed in T cells. PD1 (Programmed cell death protein 1)-integrated CAR-T cells were also demonstrated to be effective. Complete remission (CR) was achieved in seven out of eight patients (CR 87.5%). Furthermore, compared to lentivirally transduced T cells *ex vivo,* single-cell RNA sequencing demonstrated more cells with a transcriptional memory phenotype after non-viral knock-in, irrespective of the locus. Within non-virally edited cells, cells with a disrupted *PDCD1* locus showed a more robust transcriptional T cell activation signature.

Moreover, the versatility and short manufacturing time of non-virally edited T cells opens up the possibility of truly fostering the potential of neoantigen-directed TCR therapy by

integrating patient-specific TCR constructs. This was recently demonstrated by Foy et al. (2023) in a first-in-human phase 1 study. They established a clinical-grade workflow to identify personalized tumor-reactive TCRs against patient-specific mutational neoantigens. Subsequently, they used non-viral T cell engineering to knock these TCRs into the *TRAC* locus, thus placing it under endogenous transcriptional regulation and additionally disrupted the expression of the endogenous TCR β-chain. This way, therapeutic autologous T cells with up to three different personalized TCRs targeting antigens of the individual patient's tumor were manufactured and administered to 16 patients with different refractory solid cancers. They demonstrated the feasibility of scaling non-viral CRISPR-based genome editing for clinical purposes with a knock-in efficiency of 1.9% – 46.8%. Interestingly, the T cell phenotype shifted during manufacturing from predominantly T effector-like cells to mostly T_{SCM} (T memory stem cells) or T_{CM}. The safety profile of the treatment seems similarly favorable as in the previously discussed studies. TLA analysis confirmed on-target integration with no off-target integration hotspots. Similar to previous studies, *TRAC:TRBC* translocations were observed via Fluorescence in situ hybridization (FISH). One patient developed cytokine release syndrome, another grade 3 encephalitis, and all had side effects from the lymphodepletion. The best clinical response under therapy was stable disease for five patients and progressive disease for the eleven remaining patients. Analysis of biopsies from before and after treatment showed migration of the edited neoantigen-specific T cells into the tumor. Conducting a clinical study with multiple personalized TCRs per patient would not have been possible using conventional, technically cumbersome, and expensive viral T cell engineering methods.

5.4 Conclusion and Outlook

In summary, we and others have demonstrated that targeted integration of tumor-reactive TCRs in the *TRAC* locus exchanges the antigen specificity of the modified T cells, which display potent *in vitro* and *in vivo* anti-tumor functionality. The safety advantages of using the novel gene-editing approach instead of the decades-long established semi-randomly integrating vectors remain to be elucidated and will be explored further. Disruption of both endogenous TCR chains is necessary to entirely prevent competition and mispairing between the endogenous and the introduced TCR. Lastly, the functional *in vivo* advantages of using the endogenous transcriptional regulation for TCR transgenic T cells remain to be demonstrated preclinically and under clinical conditions.

A growing number of other gene editing targets are currently being explored pre-clinically and in clinical studies (reviewed by Bonini et al. (2023)). These editing targets are supposed to improve T cell function throughout the cancer-immunity cycle and the tumor microenvironment cancer-immunity subcycle (Mellman et al., 2023; Singh & Maus, 2023). Moreover, CRISPR-based loss-of-function, gain-of-function, and base-editor screens have been developed to assess the effect of individual genes, gene variants, or synthetic transgene-constructs on a diverse set of phenotypes or functional characteristics of T cells (Blaeschke et al., 2023; Carnevale et al., 2022; LaFleur et al., 2019; Schmidt et al., 2022; Schmidt et al., 2023; Schumann et al., 2020; Wei et al., 2019; Zhao et al., 2021). These screens are an unprecedented way to dissect genetic pathways underlying T cell function and dysfunction and will significantly increase our mechanistic understanding of T cell biology.

The advancement of our biological knowledge and clinical progress mutually reinforce one another: today, we can directly extract biological insights from primary human samples and the extensive clinical data gathered from patients undergoing ACT (Fraietta, Nobles, et al., 2018). At the same time, the growing mechanistic understanding of cellular decision-making and cell-cell communication within the tumor microenvironment informs new options for clinical translation (Albers & Pelka, 2022; Pulendran & Davis, 2020). Both are powered by today's unprecedented ability to genetically modify primary human T cells in a fast and precise way.

6. Attachments

6.1 Sequence of PT_2.5D6omc GeneArt Gene Strings Fragement (5’-3’)

ACTAGTGGATCAGGGGCTACTAATTTTTCCTTGCTGAAACAGGCGGGGGATGTTGAGGAAAATCCAGGGCCTATGTCTCTG
GGACTGCTGTGTTGCGGCGTGTTCAGCCTGCTGTGGGCCGGACCTGTGAATGCCGGCGTGACCCAGACCCCCAAGTTCCG
GGTGCTGAAAACCGGCCAGAGCATGACCCTGCTGTGCGCCCAGGACATGAACCACGAGTACATGTATTGGTACAGACAGGA
CCCCGGCATGGGCCTGCGGCTGATCCACTATTCTGTGGGCGAGGGCACCACCGCCAAGGGCGAAGTGCCTGATGGCTACAA
CGTGTCCCGGCTGAAGAAGCAGAACTTCCTGCTGGGCCTGGAAAGCGCCGCTCCTAGCCAGACCAGCGTGTACTTCTGCGC
CAGCAGCTACAGCAGCGGCCAGCCTCAGCACTTTGGCGACGGCACCAGACTGAGCATCCTGGAAGATCTGCGGAACGTGA
CCCCCCCCAAGGTGTCCCTGTTCGAGCCTAGCAAGGCCGAGATCGCCAACAAGCAGAAAGCCACCCTCGTGTGCCTGGCCA
GAGGCTTCTTCCCCGACCACGTGGAACTGTCTTGGTGGGTCAACGGCAAAGAGGTGCACAGCGGCGTGTGCACCGATCCC
CAGGCCTACAAAGAGAGCAACTACAGCTACTGCCTGTCCAGCAGACTGAGAGTGTCTGCCACCTTCTGGCACAACCCCCGG
AACCACTTCAGATGCCAGGTGCAGTTTCACGGCCTGAGCGAAGAGGACAAGTGGCCCGAGGGCAGCCCTAAGCCCGTGAC
ACAGAATATCAGCGCCGAAGCCTGGGGCAGAGCCGACTGTGGAATCACCAGCGCCAGCTACCATCAGGGCGTGCTGAGCG
CCACCATCCTGTACGAGATTCTGCTGGGCAAGGCCACCCTGTACGCCGTGCTGGTGTCTGGCCTGGTGCTGATGGCCATGGT
CAAGAAGAAGAACAGCGGAAGCGGCGCCACGAACTTCTCTCTGTTAAAGCAAGCAGGAGACGTGGAAGAAAACCCCGGT
CCCATGCTGCTGGAACTGATCCCCCTGCTGGGAATCCACTTCGTGCTGAGGACAGCCAGAGCCCAGTCTGTGACCCAGCCC
GACATCCACATCACCGTGTCTGAGGGCGCCAGCCTGGAACTGCGGTGCAACTACTCTTACGGCGCCACCCCCTACCTGTTTT
GGTACGTGCAGAGCCCCGGACAGGGACTGCAGCTGCTGCTGAAGTACTTTAGCGGCGACACCCTGGTGCAGGGCATCAAG
GGATTCGAGGCCGAGTTCAAGCGGAGCCAGAGCAGCTTCAACCTGCGGAAGCCCTCCGTGCATTGGAGCGACGCCGCCG
AGTATTTCTGTGCCGGCAGAGCAGCCGGCAACAAGCTGACATTTGGCGGCGGAACCAGGGTGCTCGTGAAGCCCAACATC
CAGAACCCCGAGCCCGCCGTGTACCAGCTGAAGGACCCTAGAAGCCAGGACAGCACCCTGTGCCTGTTCACCGACTTCGAC
TCCCAGATCAACGTGCCCAAGACCATGGAAAGCGGCACCTTCATCACCGACAAGTGCGTGCTGGACATGAAGGCCATGGAC
AGCAAGAGCAACGGCGCCATTGCCTGGTCCAATCAGACCAGCTTCACATGCCAGGACATCTTCAAAGAGACAAACGCCACC
TACCCCAGCAGCGACGTGCCCTGTGATGCCACCCTGACCGAGAAGTCCTTCGAGACAGACATGAATCTGAACTTCCAGAAC
CTGAGCGTGATGGGCCTGAGAATCCTGCTGCTGAAAGTGGCCGGCTTCAATCTGCTGATGACCCTGAGACTGTGGTCCAGC
TGAACGGGTGGCATCCCTGTGACCCCTCCCCAGTGCCTCTCCTGGCCCTGGAAGTTGCCACTCCAGTGCCCACCAGCCTTGT
CCTAATAAAATTAAGTTGCATCATTTTGTCTGACTAGGTGTCCTTCTATAATATTATGGGGTGGAGGGGGGTGGTATGGAGCA
AGGGGCAAGTTGGGAAGACAACCTGTAGGGCCTGCGGGGTCTATTGGGAACCAAGCTGGAGTGCAGTGGCACAATCTTG
GCTCACTGCAATCTCCGCCTCCTGGGTTCAAGCGATTCTCCTGCCTCAGCCTCCCGAGTTGTTGGGATTCCAGGCATGCATGA
CCAGGCTCAGCTAATTTTTGTTTTTTTGGTAGAGACGGGGTTTCACCATATTGGCCAGGCTGGTCTCCAACTCCTAATCTCAG
GTGATCTACCCACCTTGGCCTCCCAAATTGCTGGGATTACAGGCGTGAACCACTGCTCCCTTCCCTGTCCTTGGTAACC

7. Acknowledgments

I want to thank my supervisor, **Prof. Angela Krackhardt**, for giving me the chance to follow this project, for her excellent guidance, and for her continuous scientific and personal support to develop and follow my ideas. Thank you, Angela, for the numerous conversations, that I will remember as enriching and constructive exchanges. I have always found our dialogs to be encouraging and motivating. Thank you for actively supporting me in my scholarship applications. Your mentorship and help in advancing my scientific development means a lot to me.

This project would not have been possible without the input from so many enthusiastic and supportive colleagues. I would like to thank all the **members of the Krackhardt Lab** with whom I have had the privilege of working over the years. Especially, I want to thank **Dr. Stefan Audehm** for teaching me how to work in the lab, **Dr. Dario Gosmann** for his tireless help with the mouse work, and **Anja Ammer** for her immunohistochemistry work. Thank you, **Dr. Silvia Thoene**, **Ramona Secci**, and **Dr. Christof Winter** for the ddPCR work and for getting me hooked on data analysis. Thank you, **Anja Wolf** and **Prof. Christian Kupatt-Jeremias** for the AAV production. And thank you, **PD Katja Steiger** for the histological assessment of the mouse tissues.

I want to thank my second supervisor, **Prof. Roland Rad**, my mentor, **PD Martina Anton**, as well as **Dr. Tim Ammon**, **Dr. Rupert Öllinger**, **Prof. Dieter Saur**, **Prof. Roland Schmid**, **Prof. Marc Schmidt-Supprian**, and **Prof. Jürgen Ruland** for inspiring discussions about the project idea and findings.

I want to thank the *TUM Medical Graduate Center*, especially **Dr. Heike Blaudzun**, *ERASMUS+*, the *Max Weber-Programm,* and the *Studienstiftung des deutschen Volkes* for the generous support of the project and the several international research stays. I am very thankful that I had the opportunity to visit other exciting labs during my time in the Krackhardt Lab: Thank you, **Prof. Thomas Helleday**, **Dr. Nadilly Bonagas**, **Prof. Maurice Michel**, and **Dr. Carlos Benitez-Buelga** for showing me the overlap of DNA-Repair and Drug Development. Thank you,

Prof. Nir Hacohen and **Prof. Karin Pelka** for introducing me to a systems biology view of the immune system. Thank you **Prof. Fabian Theis** and **Giovanni Palla** for letting me dive deeper into spatial transcriptomics. Thank you **Prof. Rickard Sandberg**, **Dr. Leonard Hartmanis**, and **Prof. Christoph Ziegenhain** for showing me that transcription is more than just mean expression.

Lastly, I want to thank my **family and friends**, **Paul**, and my fiancée **Sarah**, for all the wonderful, exciting, and shaping time we experienced over all these years. Looking forward to the many more to come!

8. References

Abramson, J. S., Palomba, M. L., Gordon, L. I., Lunning, M. A., Wang, M., Arnason, J., . . . Siddiqi, T. (2020). Lisocabtagene maraleucel for patients with relapsed or refractory large B-cell lymphomas (TRANSCEND NHL 001): a multicentre seamless design study. *Lancet, 396*(10254), 839-852. doi:10.1016/S0140-6736(20)31366-0

Adikusuma, F., Piltz, S., Corbett, M. A., Turvey, M., McColl, S. R., Helbig, K. J., . . . Thomas, P. Q. (2018). Large deletions induced by Cas9 cleavage. *Nature, 560*(7717), E8-E9. doi:10.1038/s41586-018-0380-z

Ahmadi, M., King, J. W., Xue, S. A., Voisine, C., Holler, A., Wright, G. P., . . . Stauss, H. J. (2011). CD3 limits the efficacy of TCR gene therapy in vivo. *Blood, 118*(13), 3528-3537. doi:10.1182/blood-2011-04-346338

Alanis-Lobato, G., Zohren, J., McCarthy, A., Fogarty, N. M. E., Kubikova, N., Hardman, E., . . . Niakan, K. K. (2021). Frequent loss of heterozygosity in CRISPR-Cas9-edited early human embryos. *Proc Natl Acad Sci U S A, 118*(22). doi:10.1073/pnas.2004832117

Albers, J. J., Ammon, T., Gosmann, D., Audehm, S., Thoene, S., Winter, C., . . . Krackhardt, A. M. (2019). Gene editing enables T-cell engineering to redirect antigen specificity for potent tumor rejection. *Life Sci Alliance, 2*(2). doi:10.26508/lsa.201900367

Albers, J. J., & Pelka, K. (2022). Listening in on Multicellular Communication in Human Tissue Immunology. *Front Immunol, 13*, 884185. doi:10.3389/fimmu.2022.884185

Audehm, S., Glaser, M., Pecoraro, M., Braunlein, E., Mall, S., Klar, R., . . . Krackhardt, A. M. (2019). Key Features Relevant to Select Antigens and TCR From the MHC-Mismatched Repertoire to Treat Cancer. *Front Immunol, 10*, 1485. doi:10.3389/fimmu.2019.01485

Aurnhammer, C., Haase, M., Muether, N., Hausl, M., Rauschhuber, C., Huber, I., . . . Baiker, A. (2012). Universal real-time PCR for the detection and quantification of adeno-associated virus serotype 2-derived inverted terminal repeat sequences. *Hum Gene Ther Methods, 23*(1), 18-28. doi:10.1089/hgtb.2011.034

Bassani-Sternberg, M., Braunlein, E., Klar, R., Engleitner, T., Sinitcyn, P., Audehm, S., . . . Krackhardt, A. M. (2016). Direct identification of clinically relevant neoepitopes presented on native human melanoma tissue by mass spectrometry. *Nat Commun, 7*, 13404. doi:10.1038/ncomms13404

Baulu, E., Gardet, C., Chuvin, N., & Depil, S. (2023). TCR-engineered T cell therapy in solid tumors: State of the art and perspectives. *Sci Adv, 9*(7), eadf3700. doi:10.1126/sciadv.adf3700

Bausch-Fluck, D., Goldmann, U., Muller, S., van Oostrum, M., Muller, M., Schubert, O. T., & Wollscheid, B. (2018). The in silico human surfaceome. *Proc Natl Acad Sci U S A, 115*(46), E10988-E10997. doi:10.1073/pnas.1808790115

Bendle, G. M., Linnemann, C., Hooijkaas, A. I., Bies, L., de Witte, M. A., Jorritsma, A., . . . Schumacher, T. N. (2010). Lethal graft-versus-host disease in mouse models of T cell receptor gene therapy. *Nat Med, 16*(5), 565-570, 561p following 570. doi:10.1038/nm.2128

Berdeja, J. G., Madduri, D., Usmani, S. Z., Jakubowiak, A., Agha, M., Cohen, A. D., . . . Jagannath, S. (2021). Ciltacabtagene autoleucel, a B-cell maturation antigen-directed chimeric antigen receptor T-cell therapy in patients with relapsed or refractory multiple myeloma (CARTITUDE-1): a phase 1b/2 open-label study. *Lancet, 398*(10297), 314-324. doi:10.1016/S0140-6736(21)00933-8

Berdien, B., Mock, U., Atanackovic, D., & Fehse, B. (2014). TALEN-mediated editing of endogenous T-cell receptors facilitates efficient reprogramming of T lymphocytes by lentiviral gene transfer. *Gene Ther, 21*(6), 539-548. doi:10.1038/gt.2014.26

Bernard, B. E., Landmann, E., Jeker, L. T., & Schumann, K. (2022). CRISPR/Cas-based Human T cell Engineering: Basic Research and Clinical Application. *Immunol Lett, 245*, 18-28. doi:10.1016/j.imlet.2022.03.005

Blaeschke, F., Chen, Y. Y., Apathy, R., Daniel, B., Chen, A. Y., Chen, P. A., . . . Marson, A. (2023). Modular pooled discovery of synthetic knockin sequences to program durable cell therapies. *Cell, 186*(19), 4216-4234 e4233. doi:10.1016/j.cell.2023.08.013

Bonini, C., Chapuis, A. G., Hudecek, M., Guedan, S., Magnani, C., & Qasim, W. (2023). Genome Editing in Engineered T Cells for Cancer Immunotherapy. *Hum Gene Ther, 34*(17-18), 853-869. doi:10.1089/hum.2023.128

Brady, B. L., Steinel, N. C., & Bassing, C. H. (2010). Antigen receptor allelic exclusion: an update and reappraisal. *J Immunol, 185*(7), 3801-3808. doi:10.4049/jimmunol.1001158

Cappell, K. M., & Kochenderfer, J. N. (2023). Long-term outcomes following CAR T cell therapy: what we know so far. *Nat Rev Clin Oncol, 20*(6), 359-371. doi:10.1038/s41571-023-00754-1

Carnevale, J., Shifrut, E., Kale, N., Nyberg, W. A., Blaeschke, F., Chen, Y. Y., . . . Marson, A. (2022). RASA2 ablation in T cells boosts antigen sensitivity and long-term function. *Nature, 609*(7925), 174-182. doi:10.1038/s41586-022-05126-w

Cavazza, A., Moiani, A., & Mavilio, F. (2013). Mechanisms of retroviral integration and mutagenesis. *Hum Gene Ther, 24*(2), 119-131. doi:10.1089/hum.2012.203

Clauss, J., Obenaus, M., Miskey, C., Ivics, Z., Izsvak, Z., Uckert, W., & Bunse, M. (2018). Efficient Non-Viral T-Cell Engineering by Sleeping Beauty Minicircles Diminishing DNA Toxicity and miRNAs Silencing the Endogenous T-Cell Receptors. *Hum Gene Ther, 29*(5), 569-584. doi:10.1089/hum.2017.136

Cohen, C. J., Zhao, Y., Zheng, Z., Rosenberg, S. A., & Morgan, R. A. (2006). Enhanced antitumor activity of murine-human hybrid T-cell receptor (TCR) in human lymphocytes is associated with improved pairing and TCR/CD3 stability. *Cancer Res, 66*(17), 8878-8886. doi:10.1158/0008-5472.CAN-06-1450

Collins, R. H., Jr., Shpilberg, O., Drobyski, W. R., Porter, D. L., Giralt, S., Champlin, R., . . . Nemunaitis, J. (1997). Donor leukocyte infusions in 140 patients with relapsed malignancy after allogeneic bone marrow transplantation. *J Clin Oncol, 15*(2), 433-444. doi:10.1200/JCO.1997.15.2.433

Corthay, A., Nandakumar, K. S., & Holmdahl, R. (2001). Evaluation of the percentage of peripheral T cells with two different T cell receptor alpha-chains and of their potential role in autoimmunity. *J Autoimmun, 16*(4), 423-429. doi:10.1006/jaut.2001.0504

de Vree, P. J., de Wit, E., Yilmaz, M., van de Heijning, M., Klous, P., Verstegen, M. J., . . . de Laat, W. (2014). Targeted sequencing by proximity ligation for comprehensive variant detection and local haplotyping. *Nat Biotechnol, 32*(10), 1019-1025. doi:10.1038/nbt.2959

Delhove, J., & Qasim, W. (2017). Genome-Edited T Cell Therapies. *Curr Stem Cell Rep, 3*(2), 124-136. doi:10.1007/s40778-017-0077-5

Deniger, D. C., Pasetto, A., Tran, E., Parkhurst, M. R., Cohen, C. J., Robbins, P. F., . . . Rosenberg, S. A. (2016). Stable, Nonviral Expression of Mutated Tumor Neoantigen-

specific T-cell Receptors Using the Sleeping Beauty Transposon/Transposase System. *Mol Ther, 24*(6), 1078-1089. doi:10.1038/mt.2016.51

Doench, J. G., Fusi, N., Sullender, M., Hegde, M., Vaimberg, E. W., Donovan, K. F., . . . Root, D. E. (2016). Optimized sgRNA design to maximize activity and minimize off-target effects of CRISPR-Cas9. *Nat Biotechnol, 34*(2), 184-191. doi:10.1038/nbt.3437

Eyquem, J., Mansilla-Soto, J., Giavridis, T., van der Stegen, S. J., Hamieh, M., Cunanan, K. M., . . . Sadelain, M. (2017). Targeting a CAR to the TRAC locus with CRISPR/Cas9 enhances tumour rejection. *Nature, 543*(7643), 113-117. doi:10.1038/nature21405

Fagerberg, L., Jonasson, K., von Heijne, G., Uhlen, M., & Berglund, L. (2010). Prediction of the human membrane proteome. *Proteomics, 10*(6), 1141-1149. doi:10.1002/pmic.200900258

Ferrari, G., Thrasher, A. J., & Aiuti, A. (2021). Gene therapy using haematopoietic stem and progenitor cells. *Nat Rev Genet, 22*(4), 216-234. doi:10.1038/s41576-020-00298-5

Finck, A. V., Blanchard, T., Roselle, C. P., Golinelli, G., & June, C. H. (2022). Engineered cellular immunotherapies in cancer and beyond. *Nat Med, 28*(4), 678-689. doi:10.1038/s41591-022-01765-8

Foy, S. P., Jacoby, K., Bota, D. A., Hunter, T., Pan, Z., Stawiski, E., . . . Mandl, S. J. (2023). Non-viral precision T cell receptor replacement for personalized cell therapy. *Nature, 615*(7953), 687-696. doi:10.1038/s41586-022-05531-1

Fraietta, J. A., Lacey, S. F., Orlando, E. J., Pruteanu-Malinici, I., Gohil, M., Lundh, S., . . . Melenhorst, J. J. (2018). Determinants of response and resistance to CD19 chimeric antigen receptor (CAR) T cell therapy of chronic lymphocytic leukemia. *Nat Med, 24*(5), 563-571. doi:10.1038/s41591-018-0010-1

Fraietta, J. A., Nobles, C. L., Sammons, M. A., Lundh, S., Carty, S. A., Reich, T. J., . . . Melenhorst, J. J. (2018). Disruption of TET2 promotes the therapeutic efficacy of CD19-targeted T cells. *Nature, 558*(7709), 307-312. doi:10.1038/s41586-018-0178-z

Fu, Y. W., Dai, X. Y., Wang, W. T., Yang, Z. X., Zhao, J. J., Zhang, J. P., . . . Zhang, X. B. (2021). Dynamics and competition of CRISPR-Cas9 ribonucleoproteins and AAV donor-mediated NHEJ, MMEJ and HDR editing. *Nucleic Acids Res, 49*(2), 969-985. doi:10.1093/nar/gkaa1251

Govers, C., Sebestyen, Z., Coccoris, M., Willemsen, R. A., & Debets, R. (2010). T cell receptor gene therapy: strategies for optimizing transgenic TCR pairing. *Trends Mol Med, 16*(2), 77-87. doi:10.1016/j.molmed.2009.12.004

Hacein-Bey-Abina, S., Von Kalle, C., Schmidt, M., McCormack, M. P., Wulffraat, N., Leboulch, P., . . . Cavazzana-Calvo, M. (2003). LMO2-associated clonal T cell proliferation in two patients after gene therapy for SCID-X1. *Science, 302*(5644), 415-419. doi:10.1126/science.1088547

Hale, M., Lee, B., Honaker, Y., Leung, W. H., Grier, A. E., Jacobs, H. M., . . . Rawlings, D. J. (2017). Homology-Directed Recombination for Enhanced Engineering of Chimeric Antigen Receptor T Cells. *Mol Ther Methods Clin Dev, 4*, 192-203. doi:10.1016/j.omtm.2016.12.008

Hanahan, D. (2022). Hallmarks of Cancer: New Dimensions. *Cancer Discov, 12*(1), 31-46. doi:10.1158/2159-8290.CD-21-1059

Hanahan, D., & Weinberg, R. A. (2011). Hallmarks of cancer: the next generation. *Cell, 144*(5), 646-674. doi:10.1016/j.cell.2011.02.013

Harris, D. T., & Kranz, D. M. (2016). Adoptive T Cell Therapies: A Comparison of T Cell Receptors and Chimeric Antigen Receptors. *Trends Pharmacol Sci, 37*(3), 220-230. doi:10.1016/j.tips.2015.11.004

Hendel, A., Bak, R. O., Clark, J. T., Kennedy, A. B., Ryan, D. E., Roy, S., . . . Porteus, M. H. (2015). Chemically modified guide RNAs enhance CRISPR-Cas genome editing in human primary cells. *Nat Biotechnol, 33*(9), 985-989. doi:10.1038/nbt.3290

Hodgkins, A., Farne, A., Perera, S., Grego, T., Parry-Smith, D. J., Skarnes, W. C., & Iyer, V. (2015). WGE: a CRISPR database for genome engineering. *Bioinformatics, 31*(18), 3078-3080. doi:10.1093/bioinformatics/btv308

Iyer, S., Mir, A., Vega-Badillo, J., Roscoe, B. P., Ibraheim, R., Zhu, L. J., . . . Wolfe, S. A. (2022). Efficient Homology-Directed Repair with Circular Single-Stranded DNA Donors. *CRISPR J, 5*(5), 685-701. doi:10.1089/crispr.2022.0058

Jinek, M., Chylinski, K., Fonfara, I., Hauer, M., Doudna, J. A., & Charpentier, E. (2012). A programmable dual-RNA-guided DNA endonuclease in adaptive bacterial immunity. *Science, 337*(6096), 816-821. doi:10.1126/science.1225829

June, C. H., & Sadelain, M. (2018). Chimeric Antigen Receptor Therapy. *N Engl J Med, 379*(1), 64-73. doi:10.1056/NEJMra1706169

Kaeuferle, T., Stief, T. A., Canzar, S., Kutlu, N. N., Willier, S., Stenger, D., . . . Feuchtinger, T. (2022). Genome-wide off-target analyses of CRISPR/Cas9-mediated T-cell receptor engineering in primary human T cells. *Clin Transl Immunology, 11*(1), e1372. doi:10.1002/cti2.1372

Kampouri, E., Walti, C. S., Gauthier, J., & Hill, J. A. (2022). Managing hypogammaglobulinemia in patients treated with CAR-T-cell therapy: key points for clinicians. *Expert Rev Hematol, 15*(4), 305-320. doi:10.1080/17474086.2022.2063833

Kath, J., Du, W., Pruene, A., Braun, T., Thommandru, B., Turk, R., . . . Wagner, D. L. (2022). Pharmacological interventions enhance virus-free generation of TRAC-replaced CAR T cells. *Mol Ther Methods Clin Dev, 25*, 311-330. doi:10.1016/j.omtm.2022.03.018

Kierkels, G. J. J., van Diest, E., Hernandez-Lopez, P., Scheper, W., de Bruin, A. C. M., Frijlink, E., . . . Kuball, J. (2021). Characterization and modulation of anti-alphabetaTCR antibodies and their respective binding sites at the betaTCR chain to enrich engineered T cells. *Mol Ther Methods Clin Dev, 22*, 388-400. doi:10.1016/j.omtm.2021.06.011

Kim, J. H., Lee, S. R., Li, L. H., Park, H. J., Park, J. H., Lee, K. Y., . . . Choi, S. Y. (2011). High cleavage efficiency of a 2A peptide derived from porcine teschovirus-1 in human cell lines, zebrafish and mice. *PLoS One, 6*(4), e18556. doi:10.1371/journal.pone.0018556

Kim, S., Kim, D., Cho, S. W., Kim, J., & Kim, J. S. (2014). Highly efficient RNA-guided genome editing in human cells via delivery of purified Cas9 ribonucleoproteins. *Genome Res, 24*(6), 1012-1019. doi:10.1101/gr.171322.113

Klar, R., Schober, S., Rami, M., Mall, S., Merl, J., Hauck, S. M., . . . Krackhardt, A. M. (2014). Therapeutic targeting of naturally presented myeloperoxidase-derived HLA peptide ligands on myeloid leukemia cells by TCR-transgenic T cells. *Leukemia, 28*(12), 2355-2366. doi:10.1038/leu.2014.131

Klebanoff, C. A., Gattinoni, L., & Restifo, N. P. (2012). Sorting through subsets: which T-cell populations mediate highly effective adoptive immunotherapy? *J Immunother, 35*(9), 651-660. doi:10.1097/CJI.0b013e31827806e6

Kleinstiver, B. P., Pattanayak, V., Prew, M. S., Tsai, S. Q., Nguyen, N. T., Zheng, Z., & Joung, J. K. (2016). High-fidelity CRISPR-Cas9 nucleases with no detectable genome-wide off-target effects. *Nature, 529*(7587), 490-495. doi:10.1038/nature16526

Kleinstiver, B. P., Prew, M. S., Tsai, S. Q., Nguyen, N. T., Topkar, V. V., Zheng, Z., & Joung, J. K. (2015). Broadening the targeting range of Staphylococcus aureus CRISPR-Cas9 by modifying PAM recognition. *Nat Biotechnol, 33*(12), 1293-1298. doi:10.1038/nbt.3404

Kleinstiver, B. P., Prew, M. S., Tsai, S. Q., Topkar, V. V., Nguyen, N. T., Zheng, Z., . . . Joung, J. K. (2015). Engineered CRISPR-Cas9 nucleases with altered PAM specificities. *Nature, 523*(7561), 481-485. doi:10.1038/nature14592

Knies, D., Klobuch, S., Xue, S. A., Birtel, M., Echchannaoui, H., Yildiz, O., . . . Voss, R. H. (2016). An optimized single chain TCR scaffold relying on the assembly with the native CD3-complex prevents residual mispairing with endogenous TCRs in human T-cells. *Oncotarget, 7*(16), 21199-21221. doi:10.18632/oncotarget.8385

Knipping, F., Osborn, M. J., Petri, K., Tolar, J., Glimm, H., von Kalle, C., . . . Gabriel, R. (2017). Genome-wide Specificity of Highly Efficient TALENs and CRISPR/Cas9 for T Cell Receptor Modification. *Mol Ther Methods Clin Dev, 4*, 213-224. doi:10.1016/j.omtm.2017.01.005

Knott, G. J., & Doudna, J. A. (2018). CRISPR-Cas guides the future of genetic engineering. *Science, 361*(6405), 866-869. doi:10.1126/science.aat5011

Kolb, H. J., Mittermuller, J., Clemm, C., Holler, E., Ledderose, G., Brehm, G., . . . Wilmanns, W. (1990). Donor leukocyte transfusions for treatment of recurrent chronic myelogenous leukemia in marrow transplant patients. *Blood, 76*(12), 2462-2465. Retrieved from https://www.ncbi.nlm.nih.gov/pubmed/2265242

Korell, F., Berger, T. R., & Maus, M. V. (2022). Understanding CAR T cell-tumor interactions: Paving the way for successful clinical outcomes. *Med, 3*(8), 538-564. doi:10.1016/j.medj.2022.05.001

Kosicki, M., Tomberg, K., & Bradley, A. (2018). Repair of double-strand breaks induced by CRISPR-Cas9 leads to large deletions and complex rearrangements. *Nat Biotechnol, 36*(8), 765-771. doi:10.1038/nbt.4192

Krackhardt, A. M., Anliker, B., Hildebrandt, M., Bachmann, M., Eichmuller, S. B., Nettelbeck, D. M., . . . Schussler-Lenz, M. (2018). Clinical translation and regulatory aspects of CAR/TCR-based adoptive cell therapies-the German Cancer Consortium approach. *Cancer Immunol Immunother, 67*(4), 513-523. doi:10.1007/s00262-018-2119-y

Kruse, B., Buzzai, A. C., Shridhar, N., Braun, A. D., Gellert, S., Knauth, K., . . . Tuting, T. (2023). CD4(+) T cell-induced inflammatory cell death controls immune-evasive tumours. *Nature, 618*(7967), 1033-1040. doi:10.1038/s41586-023-06199-x

Kuball, J., Dossett, M. L., Wolfl, M., Ho, W. Y., Voss, R. H., Fowler, C., & Greenberg, P. D. (2007). Facilitating matched pairing and expression of TCR chains introduced into human T cells. *Blood, 109*(6), 2331-2338. doi:10.1182/blood-2006-05-023069

Labanieh, L., & Mackall, C. L. (2023). CAR immune cells: design principles, resistance and the next generation. *Nature, 614*(7949), 635-648. doi:10.1038/s41586-023-05707-3

LaFleur, M. W., Nguyen, T. H., Coxe, M. A., Yates, K. B., Trombley, J. D., Weiss, S. A., . . . Sharpe, A. H. (2019). A CRISPR-Cas9 delivery system for in vivo screening of genes in the immune system. *Nat Commun, 10*(1), 1668. doi:10.1038/s41467-019-09656-2

Legut, M., Dolton, G., Mian, A. A., Ottmann, O. G., & Sewell, A. K. (2018). CRISPR-mediated TCR replacement generates superior anticancer transgenic T cells. *Blood, 131*(3), 311-322. doi:10.1182/blood-2017-05-787598

Leibowitz, M. L., Papathanasiou, S., Doerfler, P. A., Blaine, L. J., Sun, L., Yao, Y., . . . Pellman, D. (2021). Chromothripsis as an on-target consequence of CRISPR-Cas9 genome editing. *Nat Genet, 53*(6), 895-905. doi:10.1038/s41588-021-00838-7

Leisegang, M., Engels, B., Meyerhuber, P., Kieback, E., Sommermeyer, D., Xue, S. A., . . . Uckert, W. (2008). Enhanced functionality of T cell receptor-redirected T cells is defined by the transgene cassette. *J Mol Med (Berl), 86*(5), 573-583. doi:10.1007/s00109-008-0317-3

Lessard, S., Francioli, L., Alfoldi, J., Tardif, J. C., Ellinor, P. T., MacArthur, D. G., . . . Canver, M. C. (2017). Human genetic variation alters CRISPR-Cas9 on- and off-targeting specificity at therapeutically implicated loci. *Proc Natl Acad Sci U S A, 114*(52), E11257-E11266. doi:10.1073/pnas.1714640114

Liang, X., Weigand, L. U., Schuster, I. G., Eppinger, E., van der Griendt, J. C., Schub, A., . . . Krackhardt, A. M. (2010). A single TCR alpha-chain with dominant peptide recognition in the allorestricted HER2/neu-specific T cell repertoire. *J Immunol, 184*(3), 1617-1629. doi:10.4049/jimmunol.0902155

Lim, W. A., & June, C. H. (2017). The Principles of Engineering Immune Cells to Treat Cancer. *Cell, 168*(4), 724-740. doi:10.1016/j.cell.2017.01.016

MacLeod, D. T., Antony, J., Martin, A. J., Moser, R. J., Hekele, A., Wetzel, K. J., . . . McCreedy, B. (2017). Integration of a CD19 CAR into the TCR Alpha Chain Locus Streamlines Production of Allogeneic Gene-Edited CAR T Cells. *Mol Ther, 25*(4), 949-961. doi:10.1016/j.ymthe.2017.02.005

Mall, S., Yusufi, N., Wagner, R., Klar, R., Bianchi, H., Steiger, K., . . . Krackhardt, A. M. (2016). Immuno-PET Imaging of Engineered Human T Cells in Tumors. *Cancer Res, 76*(14), 4113-4123. doi:10.1158/0008-5472.CAN-15-2784

Mayer, K. E., Mall, S., Yusufi, N., Gosmann, D., Steiger, K., Russelli, L., . . . Krackhardt, A. M. (2018). T-cell functionality testing is highly relevant to developing novel immuno-tracers monitoring T cells in the context of immunotherapies and revealed CD7 as an attractive target. *Theranostics, 8*(21), 6070-6087. doi:10.7150/thno.27275

Melenhorst, J. J., Chen, G. M., Wang, M., Porter, D. L., Chen, C., Collins, M. A., . . . June, C. H. (2022). Decade-long leukaemia remissions with persistence of CD4(+) CAR T cells. *Nature, 602*(7897), 503-509. doi:10.1038/s41586-021-04390-6

Mellman, I., Chen, D. S., Powles, T., & Turley, S. J. (2023). The cancer-immunity cycle: Indication, genotype, and immunotype. *Immunity, 56*(10), 2188-2205. doi:10.1016/j.immuni.2023.09.011

Micklethwaite, K. P., Gowrishankar, K., Gloss, B. S., Li, Z., Street, J. A., Moezzi, L., . . . Blyth, E. (2021). Investigation of product-derived lymphoma following infusion of piggyBac-modified CD19 chimeric antigen receptor T cells. *Blood, 138*(16), 1391-1405. doi:10.1182/blood.2021010858

Miller, S. M., Wang, T., Randolph, P. B., Arbab, M., Shen, M. W., Huang, T. P., . . . Liu, D. R. (2020). Continuous evolution of SpCas9 variants compatible with non-G PAMs. *Nat Biotechnol, 38*(4), 471-481. doi:10.1038/s41587-020-0412-8

Mock, U., Hauber, I., & Fehse, B. (2016). Digital PCR to assess gene-editing frequencies (GEF-dPCR) mediated by designer nucleases. *Nat Protoc, 11*(3), 598-615. doi:10.1038/nprot.2016.027

Morgan, R. A., Dudley, M. E., Wunderlich, J. R., Hughes, M. S., Yang, J. C., Sherry, R. M., . . . Rosenberg, S. A. (2006). Cancer regression in patients after transfer of genetically engineered lymphocytes. *Science, 314*(5796), 126-129. doi:10.1126/science.1129003

Müller, T. R., Jarosch, S., Hammel, M., Leube, J., Grassmann, S., Bernard, B., . . . Busch, D. H. (2021). Targeted T cell receptor gene editing provides predictable T cell product function for immunotherapy. *Cell Rep Med, 2*(8), 100374. doi:10.1016/j.xcrm.2021.100374

Nahmad, A. D., Reuveni, E., Goldschmidt, E., Tenne, T., Liberman, M., Horovitz-Fried, M., . . . Barzel, A. (2022). Frequent aneuploidy in primary human T cells after CRISPR-Cas9 cleavage. *Nat Biotechnol, 40*(12), 1807-1813. doi:10.1038/s41587-022-01377-0

Newrzela, S., Cornils, K., Li, Z., Baum, C., Brugman, M. H., Hartmann, M., . . . von Laer, D. (2008). Resistance of mature T cells to oncogene transformation. *Blood, 112*(6), 2278-2286. doi:10.1182/blood-2007-12-128751

Nguyen, D. N., Roth, T. L., Li, P. J., Chen, P. A., Apathy, R., Mamedov, M. R., . . . Marson, A. (2020). Polymer-stabilized Cas9 nanoparticles and modified repair templates increase genome editing efficiency. *Nat Biotechnol, 38*(1), 44-49. doi:10.1038/s41587-019-0325-6

Oh, S. A., Senger, K., Madireddi, S., Akhmetzyanova, I., Ishizuka, I. E., Tarighat, S., . . . Rutz, S. (2022). High-efficiency nonviral CRISPR/Cas9-mediated gene editing of human T cells using plasmid donor DNA. *J Exp Med, 219*(5). doi:10.1084/jem.20211530

Osborn, M. J., Webber, B. R., Knipping, F., Lonetree, C. L., Tennis, N., DeFeo, A. P., . . . Blazar, B. R. (2016). Evaluation of TCR Gene Editing Achieved by TALENs, CRISPR/Cas9, and megaTAL Nucleases. *Mol Ther, 24*(3), 570-581. doi:10.1038/mt.2015.197

Peng, P. D., Cohen, C. J., Yang, S., Hsu, C., Jones, S., Zhao, Y., . . . Morgan, R. A. (2009). Efficient nonviral Sleeping Beauty transposon-based TCR gene transfer to peripheral blood lymphocytes confers antigen-specific antitumor reactivity. *Gene Ther, 16*(8), 1042-1049. doi:10.1038/gt.2009.54

Poletti, V., & Mavilio, F. (2018). Interactions between Retroviruses and the Host Cell Genome. *Mol Ther Methods Clin Dev, 8*, 31-41. doi:10.1016/j.omtm.2017.10.001

Popp, M. W., & Maquat, L. E. (2016). Leveraging Rules of Nonsense-Mediated mRNA Decay for Genome Engineering and Personalized Medicine. *Cell, 165*(6), 1319-1322. doi:10.1016/j.cell.2016.05.053

Provasi, E., Genovese, P., Lombardo, A., Magnani, Z., Liu, P. Q., Reik, A., . . . Bonini, C. (2012). Editing T cell specificity towards leukemia by zinc finger nucleases and lentiviral gene transfer. *Nat Med, 18*(5), 807-815. doi:10.1038/nm.2700

Pulendran, B., & Davis, M. M. (2020). The science and medicine of human immunology. *Science, 369*(6511). doi:10.1126/science.aay4014

Rapoport, A. P., Stadtmauer, E. A., Binder-Scholl, G. K., Goloubeva, O., Vogl, D. T., Lacey, S. F., . . . June, C. H. (2015). NY-ESO-1-specific TCR-engineered T cells mediate sustained antigen-specific antitumor effects in myeloma. *Nat Med, 21*(8), 914-921. doi:10.1038/nm.3910

Robbins, P. F., Morgan, R. A., Feldman, S. A., Yang, J. C., Sherry, R. M., Dudley, M. E., . . . Rosenberg, S. A. (2011). Tumor regression in patients with metastatic synovial cell sarcoma and melanoma using genetically engineered lymphocytes reactive with NY-ESO-1. *J Clin Oncol, 29*(7), 917-924. doi:10.1200/JCO.2010.32.2537

Rosenberg, S. A., Aebersold, P., Cornetta, K., Kasid, A., Morgan, R. A., Moen, R., . . . et al. (1990). Gene transfer into humans--immunotherapy of patients with advanced

melanoma, using tumor-infiltrating lymphocytes modified by retroviral gene transduction. *N Engl J Med, 323*(9), 570-578. doi:10.1056/NEJM199008303230904

Rosenberg, S. A., Packard, B. S., Aebersold, P. M., Solomon, D., Topalian, S. L., Toy, S. T., . . . et al. (1988). Use of tumor-infiltrating lymphocytes and interleukin-2 in the immunotherapy of patients with metastatic melanoma. A preliminary report. *N Engl J Med, 319*(25), 1676-1680. doi:10.1056/NEJM198812223192527

Rosenberg, S. A., & Restifo, N. P. (2015). Adoptive cell transfer as personalized immunotherapy for human cancer. *Science, 348*(6230), 62-68. doi:10.1126/science.aaa4967

Roth, T. L., Puig-Saus, C., Yu, R., Shifrut, E., Carnevale, J., Li, P. J., . . . Marson, A. (2018). Reprogramming human T cell function and specificity with non-viral genome targeting. *Nature, 559*(7714), 405-409. doi:10.1038/s41586-018-0326-5

Ruggiero, E., Carnevale, E., Prodeus, A., Magnani, Z. I., Camisa, B., Merelli, I., . . . Bonini, C. (2022). CRISPR-based gene disruption and integration of high-avidity, WT1-specific T cell receptors improve antitumor T cell function. *Sci Transl Med, 14*(631), eabg8027. doi:10.1126/scitranslmed.abg8027

Schambach, A., Morgan, M., & Fehse, B. (2021). Two cases of T cell lymphoma following Piggybac-mediated CAR T cell therapy. *Mol Ther, 29*(9), 2631-2633. doi:10.1016/j.ymthe.2021.08.013

Schmidt, R., Steinhart, Z., Layeghi, M., Freimer, J. W., Bueno, R., Nguyen, V. Q., . . . Marson, A. (2022). CRISPR activation and interference screens decode stimulation responses in primary human T cells. *Science, 375*(6580), eabj4008. doi:10.1126/science.abj4008

Schmidt, R., Ward, C. C., Dajani, R., Armour-Garb, Z., Ota, M., Allain, V., . . . Marson, A. (2023). Base-editing mutagenesis maps alleles to tune human T cell functions. *Nature*. doi:10.1038/s41586-023-06835-6

Schober, K., Muller, T. R., & Busch, D. H. (2020). Orthotopic T-Cell Receptor Replacement-An "Enabler" for TCR-Based Therapies. *Cells, 9*(6). doi:10.3390/cells9061367

Schober, K., Muller, T. R., Gokmen, F., Grassmann, S., Effenberger, M., Poltorak, M., . . . Busch, D. H. (2019). Orthotopic replacement of T-cell receptor alpha- and beta-chains with preservation of near-physiological T-cell function. *Nat Biomed Eng, 3*(12), 974-984. doi:10.1038/s41551-019-0409-0

Scholler, J., Brady, T. L., Binder-Scholl, G., Hwang, W. T., Plesa, G., Hege, K. M., . . . June, C. H. (2012). Decade-long safety and function of retroviral-modified chimeric antigen receptor T cells. *Sci Transl Med, 4*(132), 132ra153. doi:10.1126/scitranslmed.3003761

Scholten, K. B., Kramer, D., Kueter, E. W., Graf, M., Schoedl, T., Meijer, C. J., . . . Hooijberg, E. (2006). Codon modification of T cell receptors allows enhanced functional expression in transgenic human T cells. *Clin Immunol, 119*(2), 135-145. doi:10.1016/j.clim.2005.12.009

Schumacher, T. N., Scheper, W., & Kvistborg, P. (2019). Cancer Neoantigens. *Annu Rev Immunol, 37*, 173-200. doi:10.1146/annurev-immunol-042617-053402

Schumann, K., Lin, S., Boyer, E., Simeonov, D. R., Subramaniam, M., Gate, R. E., . . . Marson, A. (2015). Generation of knock-in primary human T cells using Cas9 ribonucleoproteins. *Proc Natl Acad Sci U S A, 112*(33), 10437-10442. doi:10.1073/pnas.1512503112

Schumann, K., Raju, S. S., Lauber, M., Kolb, S., Shifrut, E., Cortez, J. T., . . . Marson, A. (2020). Functional CRISPR dissection of gene networks controlling human regulatory T cell identity. *Nat Immunol, 21*(11), 1456-1466. doi:10.1038/s41590-020-0784-4

Scully, R., Panday, A., Elango, R., & Willis, N. A. (2019). DNA double-strand break repair-pathway choice in somatic mammalian cells. *Nat Rev Mol Cell Biol, 20*(11), 698-714. doi:10.1038/s41580-019-0152-0

Seki, A., & Rutz, S. (2018). Optimized RNP transfection for highly efficient CRISPR/Cas9-mediated gene knockout in primary T cells. *J Exp Med, 215*(3), 985-997. doi:10.1084/jem.20171626

Shy, B. R., Vykunta, V. S., Ha, A., Talbot, A., Roth, T. L., Nguyen, D. N., . . . Marson, A. (2023). High-yield genome engineering in primary cells using a hybrid ssDNA repair template and small-molecule cocktails. *Nat Biotechnol, 41*(4), 521-531. doi:10.1038/s41587-022-01418-8

Singh, N., & Maus, M. V. (2023). Synthetic manipulation of the cancer-immunity cycle: CAR-T cell therapy. *Immunity, 56*(10), 2296-2310. doi:10.1016/j.immuni.2023.09.010

Slaymaker, I. M., Gao, L., Zetsche, B., Scott, D. A., Yan, W. X., & Zhang, F. (2016). Rationally engineered Cas9 nucleases with improved specificity. *Science, 351*(6268), 84-88. doi:10.1126/science.aad5227

Sommermeyer, D., & Uckert, W. (2010). Minimal amino acid exchange in human TCR constant regions fosters improved function of TCR gene-modified T cells. *J Immunol, 184*(11), 6223-6231. doi:10.4049/jimmunol.0902055

Stadtmauer, E. A., Fraietta, J. A., Davis, M. M., Cohen, A. D., Weber, K. L., Lancaster, E., . . . June, C. H. (2020). CRISPR-engineered T cells in patients with refractory cancer. *Science, 367*(6481). doi:10.1126/science.aba7365

Stronen, E., Toebes, M., Kelderman, S., van Buuren, M. M., Yang, W., van Rooij, N., . . . Schumacher, T. N. (2016). Targeting of cancer neoantigens with donor-derived T cell receptor repertoires. *Science, 352*(6291), 1337-1341. doi:10.1126/science.aaf2288

Takata, M., Sasaki, M. S., Sonoda, E., Morrison, C., Hashimoto, M., Utsumi, H., . . . Takeda, S. (1998). Homologous recombination and non-homologous end-joining pathways of DNA double-strand break repair have overlapping roles in the maintenance of chromosomal integrity in vertebrate cells. *EMBO J, 17*(18), 5497-5508. doi:10.1093/emboj/17.18.5497

Tipanee, J., VandenDriessche, T., & Chuah, M. K. (2017). Transposons: Moving Forward from Preclinical Studies to Clinical Trials. *Hum Gene Ther, 28*(11), 1087-1104. doi:10.1089/hum.2017.128

Tsuchida, C. A., Brandes, N., Bueno, R., Trinidad, M., Mazumder, T., Yu, B., . . . Doudna, J. A. (2023). Mitigation of chromosome loss in clinical CRISPR-Cas9-engineered T cells. *Cell, 186*(21), 4567-4582 e4520. doi:10.1016/j.cell.2023.08.041

Uhlen, M., Fagerberg, L., Hallstrom, B. M., Lindskog, C., Oksvold, P., Mardinoglu, A., . . . Ponten, F. (2015). Tissue-based map of the human proteome. *Science, 347*(6220), 1260419. doi:10.1126/science.1260419

Untergasser, A., Nijveen, H., Rao, X., Bisseling, T., Geurts, R., & Leunissen, J. A. (2007). Primer3Plus, an enhanced web interface to Primer3. *Nucleic Acids Res, 35*(Web Server issue), W71-74. doi:10.1093/nar/gkm306

Vakulskas, C. A., Dever, D. P., Rettig, G. R., Turk, R., Jacobi, A. M., Collingwood, M. A., . . . Behlke, M. A. (2018). A high-fidelity Cas9 mutant delivered as a ribonucleoprotein complex enables efficient gene editing in human hematopoietic stem and progenitor cells. *Nat Med, 24*(8), 1216-1224. doi:10.1038/s41591-018-0137-0

van Loenen, M. M., de Boer, R., Amir, A. L., Hagedoorn, R. S., Volbeda, G. L., Willemze, R., . . . Heemskerk, M. H. (2010). Mixed T cell receptor dimers harbor potentially harmful

neoreactivity. *Proc Natl Acad Sci U S A, 107*(24), 10972-10977. doi:10.1073/pnas.1005802107

Waldman, A. D., Fritz, J. M., & Lenardo, M. J. (2020). A guide to cancer immunotherapy: from T cell basic science to clinical practice. *Nat Rev Immunol, 20*(11), 651-668. doi:10.1038/s41577-020-0306-5

Walton, R. T., Christie, K. A., Whittaker, M. N., & Kleinstiver, B. P. (2020). Unconstrained genome targeting with near-PAMless engineered CRISPR-Cas9 variants. *Science, 368*(6488), 290-296. doi:10.1126/science.aba8853

Wang, D., Tai, P. W. L., & Gao, G. (2019). Adeno-associated virus vector as a platform for gene therapy delivery. *Nat Rev Drug Discov, 18*(5), 358-378. doi:10.1038/s41573-019-0012-9

Wang, J. Y., & Doudna, J. A. (2023). CRISPR technology: A decade of genome editing is only the beginning. *Science, 379*(6629), eadd8643. doi:10.1126/science.add8643

Wang, Y., Wang, B., Xie, H., Ren, Q., Liu, X., Li, F., . . . Gu, F. (2019). Efficient Human Genome Editing Using SaCas9 Ribonucleoprotein Complexes. *Biotechnol J, 14*(7), e1800689. doi:10.1002/biot.201800689

Wei, J., Long, L., Zheng, W., Dhungana, Y., Lim, S. A., Guy, C., . . . Chi, H. (2019). Targeting REGNASE-1 programs long-lived effector T cells for cancer therapy. *Nature, 576*(7787), 471-476. doi:10.1038/s41586-019-1821-z

Wienert, B., & Cromer, M. K. (2022). CRISPR nuclease off-target activity and mitigation strategies. *Front Genome Ed, 4*, 1050507. doi:10.3389/fgeed.2022.1050507

Wienert, B., Nguyen, D. N., Guenther, A., Feng, S. J., Locke, M. N., Wyman, S. K., . . . Corn, J. E. (2020). Timed inhibition of CDC7 increases CRISPR-Cas9 mediated templated repair. *Nat Commun, 11*(1), 2109. doi:10.1038/s41467-020-15845-1

Yusufi, N., Mall, S., Bianchi, H. O., Steiger, K., Reder, S., Klar, R., . . . D'Alessandria, C. (2017). In-depth Characterization of a TCR-specific Tracer for Sensitive Detection of Tumor-directed Transgenic T Cells by Immuno-PET. *Theranostics, 7*(9), 2402-2416. doi:10.7150/thno.17994

Zhang, J., Hu, Y., Yang, J., Li, W., Zhang, M., Wang, Q., . . . Huang, H. (2022). Non-viral, specifically targeted CAR-T cells achieve high safety and efficacy in B-NHL. *Nature, 609*(7926), 369-374. doi:10.1038/s41586-022-05140-y

Zhang, X. H., Tee, L. Y., Wang, X. G., Huang, Q. S., & Yang, S. H. (2015). Off-target Effects in CRISPR/Cas9-mediated Genome Engineering. *Mol Ther Nucleic Acids, 4*(11), e264. doi:10.1038/mtna.2015.37

Zhao, H., Liu, Y., Wang, L., Jin, G., Zhao, X., Xu, J., . . . Peng, M. (2021). Genome-wide fitness gene identification reveals Roquin as a potent suppressor of CD8 T cell expansion and anti-tumor immunity. *Cell Rep, 37*(10), 110083. doi:10.1016/j.celrep.2021.110083

Ziegler, T., Kraus, M., Husada, W., Gesenhues, F., Jiang, Q., Pinkenburg, O., . . . Hinkel, R. (2017). Steerable Induction of the Thymosin beta4/MRTF-A Pathway via AAV-Based Overexpression Induces Therapeutic Neovascularization. *Hum Gene Ther*. doi:10.1089/hum.2017.013